IEEE Access
Multidisciplinary | Rapid Review | Open Access Journal

Received 1 July 2023, accepted 31 July 2023, date of publication 7 August 2023, date of current version 25 August 2023.

*Digital Object Identifier 10.1109/ACCESS.2023.3302696*

RESEARCH ARTICLE

# Improved Particle Filter-Based Modeling With Robotic GMAW for Weld Forming Prediction

**ZIQUAN JIAO[1,2], XINGYU GAO[1], ZHIQIANG FENG[2], TONGSHUAI YANG[2], SHANBEN CHEN[3], (Senior Member, IEEE), AND WENJING LIU[4]**

[1]School of Mechanical and Electrical Engineering, Guilin University of Electronic Technology, Guilin 541004, China
[2]Guangxi Engineering Technology Research Center of Ship Digital Design and Advanced Manufacturing, Beibu Gulf University, Qinzhou 535011, China
[3]Intelligentized Robotic Welding Technology Laboratory, Shanghai Jiao Tong University, Shanghai 200240, China
[4]Faculty of Education, Saitama University, Saitama 338-8570, Japan

Corresponding author: Xingyu Gao (sjtufjzq@sina.com)

This work was supported in part by the National Natural Science Foundation of China under Grant 51969001 and Grant 52261044, in part by the Guangxi Innovation-Driven Development Special Fund Project of China under Grant GuikeAA18118002-3, in part by the Guangxi Natural Science Foundation of China under Grant 2021GXNSFBA075023 and Grant 2018JJA170110, in part by the Guangxi Science and Technology Plan Project of China under Grant GuikeAD18281007, and in part by the Innovation Project of Guangxi Graduate Education under Grant YCBZ2019050 and Grant 2020YCXB01.

**ABSTRACT** To solve the knowledge modelling problem of strong nonlinear characteristics such as multivariable, high coupling and stochastic interference in the GMAW process of hull structures, a clustering similarity particle filter (CSPF) method based on the consistency principle of the state trajectory is proposed to establish a knowledge model for welding dynamics. The modelling mechanism of the stochastic process is selected to construct a Hammerstein model with uncertain noise in the relationship between the welding parameters and geometric characteristics of the weld pool, and the Hammerstein model is identified using a step response test of constant specification and two parameter identification algorithms: the recursive least squares method and the final prediction error criterion. Thus, the state space equation of the accurate identification structure is provided for knowledge process modelling. Relying on the particle filter algorithm as the core of the modelling framework and theoretical analysis, *SIS* filtering and *GPF* prediction methods are adopted to obtain the combined trajectory formed by the current (original) and future multistage (modified) spatial state information, and the state similarity between the combined trajectory and the actual system trajectory is measured by the cluster analysis method. A new proposed distribution is generated under the guidance of similarity measurement to improve the particle degradation phenomenon, update the first-order Markov process with new observation information to compensate and modify the importance weight calculation, replace the resampling strategy to eliminate the particle depletion problem, and then establish the welding knowledge model of state tracking and forming prediction. Through simulation and experimentation of hull structure GMAW, it is concluded that both the training effect of state tracking and the prediction accuracy of weld formation can meet the process requirements of ship welding by particle filter and its improved method. Meanwhile, integrated with the convergence theorem of the CSPF algorithm, compared with the standard particle filter and auxiliary particle filter, the training effect of state tracking is better in the application of the CSPF method in the process knowledge modelling of hull structure GMAW, and the prediction results of weld forming have the advantages of higher accuracy, stronger robustness, and better timeliness.

**INDEX TERMS** Particle filter, robotic GMAW, weld forming prediction, Bayesian theory, Markov process, clustering similarity.

## I. INTRODUCTION

As an important part of modern shipbuilding technology, gas metal arc welding (GMAW) using intelligent robots has received increasing attention from marine engineers [1], [2], [3]. The traditional GMAW process for hull structures mainly depends on manual operations by experienced technicians. However, it has the shortcomings of high welder labour intensity, low production efficiency and difficulty in ensuring product quality, which promotes the transition of ship welding manufacturing from manual operation to automation, robotics and intelligence. The premise of realizing the

The associate editor coordinating the review of this manuscript and approving it for publication was Usama Mir.

intelligent requirements of ship GMAW technology is to be able to describe and master the knowledge of various welding states, that is, the knowledge modelling of the welding dynamic process [4], [5]. The purpose is to raise welding phenomena to their essence, determine the trends and characteristics representing different welding behaviours, upgrade it from technology to science, and provide theoretical and technical support for the development of welding automation and intelligence.

However, the knowledge modelling of ship GMAW describes the relationship between process parameters and forming characteristics, which is generally expressed in the theoretical form of physics or mathematics, and the accuracy of the model seriously depends on the degree of understanding welding requirements [6]. Aiming at the unmeasurable problem of forming prediction, it is usually necessary to establish a mapping relationship between the welding specification parameters and weld forming characteristics, that is, knowledge modelling of the welding dynamic process. At present, the research on welding process modelling mainly includes three categories: numerical simulation, weld pool vibration method and geometric characteristic modelling. Numerical simulation [7], [8] uses a numerical analysis method to calculate the physical law of the heat flow field of a weld pool and the surrounding environment during the welding process according to some theoretical assumptions and then establishes the corresponding relationship with the welding parameters, such as the temperature field model [9], penetration and weld pool surface contour model [10], plasma arc model [11], etc. Although the model has high prediction accuracy under the premise of theoretical assumptions, it can only be used in off-line process because of its poor description and large amount of calculation for complex and changeable welding dynamic process. The weld pool vibration method assumes that the weld pool can be represented by a mathematical model with uncertain parameters and a determined model structure. According to the deterministic relationship between the inherent oscillation frequency and model parameters, the unknown parameters of the weld pool model can be determined by measuring the oscillation frequency of the weld pool. Kotecki [12] first pointed out that the change in arc force caused by welding current can cause the weld pool to vibrate, including the oscillation of the weld pool at a natural frequency after arc termination. Wang et al. [13] found that a current superimposed with an AC signal of a certain frequency during DC welding will cause a periodic change in the arc force, causing vibration on the surface of the weld pool, and then obtained the corresponding relationship between the weld pool size and vibration frequency. On the premise of specific welding methods, this method can ensure a high accuracy level of penetration prediction, but it requires a variety of specific measurement sensors, which has certain application limitations.

The characteristic modelling of weld pool geometry is an important premise to ensure welding quality. However, in practical engineering applications, due to the complexity of the ship structure and various processes and limited by the environmental conditions, it is difficult to directly observe the geometric characteristics of the weld pool in real time, such as the front weld width, reinforcement, weld depth, etc. Many engineering practices and welder experiences [14], [15] show that there is a correlation between the geometric characteristics of the weld pool and the welding process parameters. Through the adjustment of the process parameters, the geometric characteristics of the weld pool can be predicted and controlled. This paper mainly studies the knowledge modelling method of ship intelligent GMAW, which belongs to the above classification. At the same time, with the development of artificial intelligence technology, such as neural networks, support vector machines, fuzzy sets, and rough sets, an increasing number of scholars have introduced artificial intelligence modelling methods into the prediction and control of welding dynamic process. The dynamic process of ship GMAW has the characteristics of strong nonlinearity, continuity, time-delay, multivariable coupling, uncertain factors and stochastic interference. An artificial intelligence method can well describe the whole welding process to a certain extent. Li and Amith et al. [16], [17] established an artificial neural network prediction model based on the relationship between welding process parameters (peak current, welding speed, wire filler rate, etc.) and the geometric characteristics of the weld pool. Chen and Feng [18], [19], [20], [21] fully obtained welding experience knowledge and established a knowledge model of the ship welding process by extracting fuzzy set and rough set rules using a support vector machine to solve the problem of predicting the geometric characteristics of the weld pool.

Although the above methods have made great research progress, due to the operation requirements of these methods, it is necessary to discretize the continuity of the welding dynamic process and learn from a large amount of prior knowledge, resulting in the inclusion of more subjective factors in the modelling method, which affects the accuracy of the results [22]. Meanwhile, the mathematical model established using the above method is based on deterministic system theory, and the relationship between input and output strictly corresponds. In the process of obtaining parameter output according to the model, the influence of system interference in the process is generally not considered. The influence of system interference in the process of obtaining parameter output according to the model is generally not considered [23]. While the particle filter method selected in this paper is to realize Bayesian state estimation through Monte Carlo simulation technology. The Hammerstein stochastic noise model is used to construct the state space equation, which determines the objective change rule of welding process parameters and weld formation. Combined with the particle degradation and depletion problems existing in conventional particle filter, a cluster similarity particle filter is used to establish the dynamic knowledge model of

ship GMAW process under the joint action of multivariable coupling and stochastic interference factors, which can effectively solve the strong nonlinear problem of continuity, time-delay and stochastic interference in ship GMAW, and makes up for the defects of prior knowledge and stochastic noise.

The paper is structured as follows. In Section II, we present the background knowledge theory of ship GMAW dynamic process. Section III presents the modelling and application of a particle filter for ship GMAW and provides a theoretical explanation of the CSPF and proves the relevant theorems. In Section IV, the CSPF simulation results of state tracking and form prediction are compared with other PF algorithms. Finally, conclusions are drawn in Section V.

## II. KNOWLEDGE MODELING OF SHIP GMAW DYNAMIC PROCESS

There are many types of stochastic disturbances with uncertain characteristics in the ship GMAW process, such as unstable output of power supply, changes in weld gap, environmental temperature fluctuations, thermal deformation and accumulation, etc., which can cause uncertainty in the actual operation of the welding system, resulting in the solid state forming of the weld pool changing with stochastic noise under constant process parameter input. At present, artificial intelligence methods are mainly based on deterministic system theory, and the relationship between parameter inputs and response outputs is strictly corresponding, without considering the influence of time-varying processes and stochastic disturbances in welding systems. Knowledge modelling issues related to ship GMAW nonlinearity, time-delay, multivariable coupling, and stochastic disturbances, this paper selects the stochastic mechanism to abstract the welding dynamic system, which will be more suitable for the actual process. Based on this, the Hammerstein stochastic noise model is introduced to establish the nonlinear mapping relationship between welding specification parameters and weld pool shape, which accurately reflects the characteristic effect of stochastic noise in the actual production process. And then the noise model structure is identified and optimized by step response test, recursive least squares and final prediction error criterion to obtain the state space equation representing the GMAW dynamic physical process, which determines the objective change rule of welding process parameters and weld formation.

To solve the problem of nonlinear knowledge modelling of ship GMAW, the process characteristics should be understood. Process parameters and the material state are two important factors affecting the characteristic parameters of the weld pool during dynamic welding. Among them, the process parameters include the welding current, arc voltage, wire filler rate and welding speed, and the material state includes the welding plate and weld gap. To fully understand the dynamic change trend of weld pool characteristics with different welding processes in the ship welding process, a state space mathematical model between the welding specification parameters and weld pool shape characteristics is established using the principle of stochastic process modelling, and then the model structure and parameters are identified according to online identification technology. Finally, combined with the clustering similarity particle filter, the characteristic parameters of the weld pool are predicted, which provides a technical basis for weld forming quality control in the ship GMAW welding process.

### A. STOCHASTIC VARIABLES AND NOISE INTERFERENCE IN THE SHIP GMAW PROCESS

Assuming that various process conditions are in an ideal state, such as standardized plate form, constant weld gap, stable gas flow and heat dissipation conditions, maintained working environment temperature and no noise interference, a stable welding process can be obtained using constant standardized welding parameters to ensure the stability and quality of weld formation. However, in an actual ship welding working environment, the above working conditions (including the welding specification parameters) are unstable and unpredictable. The stochastic property of this working condition affects the stability of the welding process, making the welding results stochastic. In the process of system identification parameters and knowledge modelling, process parameter data are collected using measuring instruments in the dynamic welding, but the measured values are inaccurate due to noise interference error.

The action of interference noise on knowledge modelling can be divided into deterministic interference and stochastic interference noise [24]. Deterministic interference noise can be expressed as

$$\mathbb{Z}_d(t) = T(t) + \psi(t) \tag{1}$$

where $\mathbb{Z}_d$, $T$ and $\psi$ are the measured value, true value and interference noise of the system, respectively. Stochastic interference noise can be expressed as

$$\mathbb{Z}_r(t) = f[T(t), \Psi(t)] \tag{2}$$

where the mixed signal $\mathbb{Z}_r$ is a nonadditive function of $T$ and $\Psi$. These disturbances cause some process parameters in the welding dynamic system to become stochastic variables. Only when the stochastic process is introduced into the welding dynamic modelling can the characteristics and effects of the stochastic noise in the actual welding process be truly reflected.

### B. STOCHASTIC PROCESS MODELING PRINCIPLE OF SHIP GMAW

GMAW is a heat treatment process in which hull structural materials undergo heating, melting, solidification and continuous cooling under the action of an arc heat source. According to the theory of heat transfer, arc heat can be regarded as the excitation of a dynamic system, which is a static nonlinear functional relationship, and the heat transfer process can be approximated by a dynamic linear system. For the welding process that can be decomposed into nonlinear

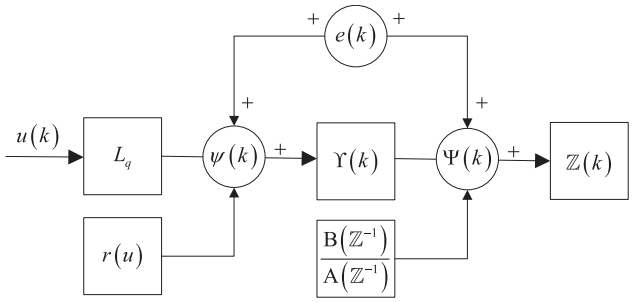


**FIGURE 1.** Hammerstein stochastic noise model for hull structure GMAW.

and linear subsystems, we use a Hammerstein model [25] for simulation as shown in Figure 1.

In Figure 1, $L_q = q^{-d}$ is the time translation operator of the delay factor, and $d$ is the time-delay factor. The zero memory nonlinearity factor is $\Upsilon(k) = \gamma_1 u + \gamma_2 u^2 + \cdots + \gamma_p u^p + \psi(k)$ and the linear dynamic subsystem is

$$\frac{B(\mathbb{Z}^{-1})}{A(\mathbb{Z}^{-1})} = \frac{\beta_1 \mathbb{Z}^{-1} + \beta_2 \mathbb{Z}^{-2} + \cdots + \beta_n \mathbb{Z}^{-l}}{\alpha_1 \mathbb{Z}^{-1} + \alpha_2 \mathbb{Z}^{-2} + \cdots + \alpha_n \mathbb{Z}^{-l}} \tag{3}$$

where $u(k)$ and $\mathbb{Z}(k)$ are the input and actual output variables of the system process, respectively and $\gamma(u)$ and $\Upsilon(k)$ are the input functions and output variables of the nonlinear factor. The equivalent synthetic noise is $e(k) = \Psi(k) + \psi(k)/A(\mathbb{Z})$, $\psi(k)$ and $\Psi(k)$ are distributed noise in different stages of the nonlinear factor and linear part, respectively.

There are many sources of interference noise in the actual welding process. During model construction, all the stochastic noise effects are integrated together and replaced by an equivalent noise. The model in Figure 1 can be simplified to the following time domain expression:

$$A(q^{-1})\mathbb{Z}(k) = B(q^{-1}) \sum_{i=1}^{p} \gamma_i u^i (k-d) + e(k) \tag{4}$$

Further expansion can be obtained as follows:

$$\begin{aligned} \mathbb{Z}(k) = &- \sum_{i=1}^{l} \alpha_i \mathbb{Z}(k-i) \\ &+ \sum_{i=0}^{m} \sum_{j=1}^{p} \beta_i \gamma_j u^j (k-j-d) + e(k) \end{aligned} \tag{5}$$

Let

$$\begin{aligned} \Gamma(k) = [&-\mathbb{Z}(k-1), -\mathbb{Z}(k-2), \ldots, -\mathbb{Z}(k-l), u(k-d), \\ &u(k-d-1), \ldots, u(k-d-m), u^2(k-d), \\ &u^2(k-d-1), \ldots, u^2(k-d-m), u^p(k-d), \\ &u^p(k-d-1), \ldots, u^p(k-d-m)] \end{aligned} \tag{6}$$

$$\begin{aligned} \vartheta = [&\alpha_1, \alpha_2, \cdots, \alpha_l, \beta_0\gamma_1, \beta_1\gamma_1, \cdots, \beta_m\gamma_1, \beta_0\gamma_2, \beta_1\gamma_2, \\ &\cdots, \beta_m\gamma_2, \beta_0\gamma_p, \beta_1\gamma_p, \cdots, \beta_m\gamma_p]^T \end{aligned} \tag{7}$$

Then, the above formula can be rewritten as

$$\mathbb{Z}(k) = \Gamma(k)\vartheta + e(k) \tag{8}$$

where $\Gamma(k) : 1 \times [l + p \times (m + 1)]$ is a dimension vector, $\vartheta : [l + p \times (m + 1)] \times 1$ is a dimension vector, $l, m$ are the order of the linear dynamic subsystem, $p, d$ are the highest power and time-delay factor of the nonlinear part, $\Gamma, \vartheta$ are the model structure and parameters, respectively.

### C. STRUCTURE IDENTIFICATION OF THE HAMMERSTEIN STOCHASTIC NOISE MODEL

Model structure identification is the premise and guarantee of welding forming prediction. In system identification, there are many selection methods for structural parameter estimation [26], such as the Akaike criterion, rank estimation of the Hankel matrix, determinant ratio, variance estimation of residuals, recursive least squares method (RLS), final prediction error criterion (FPE) and so on. In this paper, under the reasonable design of an identification test, the structural parameters of the Hammerstein stochastic noise model are estimated as the combination of the step response, RLS and FPE. First, the step response identification method is used to determine the time-delay factor. Second, assuming the order of the linear subsystem, the optimal highest power of the nonlinear part is obtained using the RLS method [27]. Finally, the FPE criterion [28] is used to evaluate the optimal linear order selection. In this example, the welding current and wire filler rate are selected as the input parameters to the model, and the geometric dimension characteristics of the weld pool represented by the weld width are used as the input parameters.

The step signal is simple and easy to obtain, and its response reflects the main information of the welding dynamic characteristics and can also be used as the input signal for system identification. Methods to determine the process transfer function using the step response include the approximation method, semilogarithm method, tangent method, two-point method and area method [29]. In this paper, the more mature area method is used for step response identification. The specific steps are as follows: a) Design step response process test to obtain input and output data; b) Necessary preprocessing of data: simplification and screening; c) Draw the model response curve and verify the model; d) The identified discrete model is transformed into the expression of a continuous transfer function; e) The time-delay factor of the model is determined according to the welding empirical knowledge and transfer function.

The material selected for the step response test is low carbon steel Q235. The most commonly used carbon dioxide gas shielded welding for hull construction is selected for GMAW welding. The welding process is flat butt welding. The process parameters of the welding specification are determined through the rule database: the welding current $I$ ranges from 120 A to 170 A, the arc voltage $V_A = 20$ V, the welding speed $V_W = 2.5$ mm/s and the plate frame gap $g = 4.0$ mm. In the current step test, the arc voltage $V_A$ and welding speed $V_W$ remain unchanged. The positive/negative step of the welding current is 50 A, from 120 A to 170 A,

and the negative step value is from 170 A to 120 A. In the welding process, after 60 sampling points are collected with the initial current, the step change is generated by the current controller. From the 61st sampling point as the output result after the step response, the characteristic parameters of the weld width and welding current are obtained using the weld pool image and a current sensing system. Using the same identification method, the transfer function under the condition of a negative current step can be obtained. The specific current step response is shown in Figure 2.

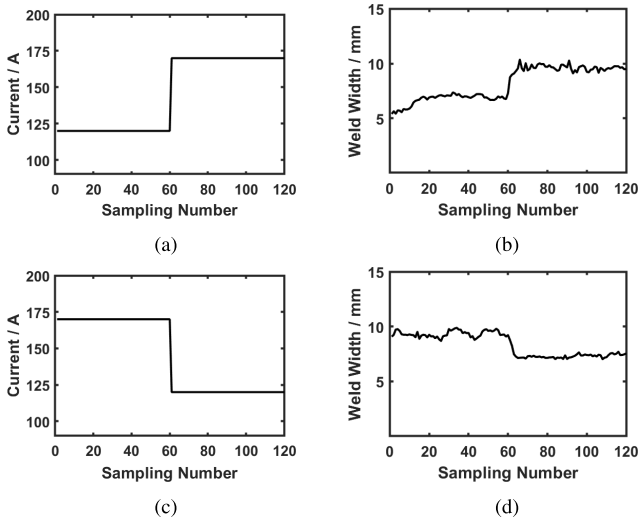


**FIGURE 2.** Transient response of weld width with current step. (a) Current of positive step (b) Weld width of positive step (c) Current of negative step (d) Weld width of negative step.

The determination of the time-delay factor is related to the transfer function of the step response. From the distribution of data shown in Figure 2, there is no oscillation phenomenon in the welding process under the current step response. Therefore, it can be considered a first-order system, and its transfer function is as follows:

$$G(s) = \frac{Ke^{-ds}}{1 + ts} \tag{9}$$

where $K$ is the gain coefficient of the step response and $t$ is the time constant. Since the structural order of the system transfer function has been determined, the minimum condition parameters of the degree of fitting and comprehensive error FPE are compared and selected as the time-delay factor, and then other characteristic parameters of the transfer function are determined. Since the structural order of the system transfer function has been determined, the optimal condition parameters of the degree of fitting and comprehensive error FPE are compared and selected as the time-delay factor, and then the other characteristic parameters of the transfer function are determined. The transfer function parameters of the shape characteristics of the weld pool with positive/negative current steps are shown in Table 1.

According to the identification results shown in Table 1, the time-delay characteristics of the weld width $W_f$ response

**TABLE 1.** Transfer function parameters of weld shape characteristics under current step response.

| Weld shape characteristic | | Positive step | Negative step |
|---|---|---|---|
| Weld width | Time constant $t$ | 1.608 | 1.463 |
| | Gain coefficient $K$ | 0.057 | 0.040 |
| | Time-delay factor $d$ | 0.467 | 0.149 |
| | Degree of fitting | 83.38% | 84.58% |
| | FPE | 0.070 | 0.029 |

under positive and negative step conditions are not obvious, while the time-delay factor $d$ of the weld width under positive step conditions is larger than that under negative step conditions, indicating that low carbon steel weld forming is more sensitive to a reduction in heat input than an increase in equivalent heat input. Under the condition of a positive step, the gain coefficient $K$ and time constant $t$ of the weld width are larger than that of a negative step, which shows that the weld forming is not only determined by the heat input but also affected by the arc thrust. With a decrease in current, the arc thrust decreases rapidly, resulting in a rapid change in weld forming characteristics. In the positive and negative step tests, the parameters of the transfer function obtained are different, indicating that the welding process has the characteristics of nonlinearity, strong coupling and variable time delay. Therefore, the above influencing factors should be fully considered in the knowledge modelling of the hull GMAW process.

In the GMAW process of a hull structure, the wire filler rate and its determined wire filling amount are very important to weld forming. A change in the wire filling amount will directly lead to a change in the weld width and reinforcement characteristics. When the wire diameter, feeding and swing mode of the welding gun are determined, only the wire filler rate can determine the wire filler effect. Therefore, the wire filler rate should be considered as an important influencing factor of weld forming in the knowledge modelling of the welding process. In this case, the wire filler rate $V_F$ is selected from 2.6 to 4.5 m/min, and other welding process parameters refer to the current step test. In the welding process, after 60 sampling points are collected with the initial wire filler rate, a step change of 1.9 m/min is generated by the filler controller. From the 61st sampling point as the output result after the step response, the characteristic parameters of the weld width and filler rate are obtained using the weld pool image and a wire sensing system. Using the same identification method, the transfer function under the condition of a negative step can be obtained. The specific step response of the wire filler rate is shown in Figure 3.

From the data distribution shown in Figure 3, it can be seen that the step response of the wire filler rate has a similar function structure with the step of the welding current. Using a similar identification method, the transfer function parameters of the shape characteristics of the weld pool with positive and negative wire filler rate steps are shown in Table 2.

According to the transfer function identification results shown in Table 2, the time-delay characteristics of the

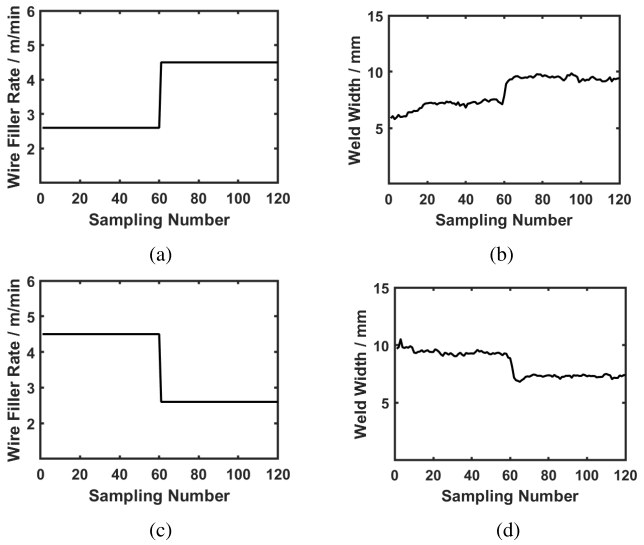


**FIGURE 3.** Transient response of weld width with wire filler rate step. (a) Wire filler rate of positive step (b) Weld width of positive step (c) Wire filler rate of negative step (d) Weld width of negative step.

**TABLE 2.** Transfer function parameters of weld shape characteristics under wire filler rate step response.

| Weld shape characteristic | | Positive step | Negative step |
|---|---|---|---|
| Weld width | Time constant $t$ | 3.483 | 0.219 |
| | Gain coefficient $K$ | 0.731 | 0.982 |
| | Time-delay factor $d$ | 0 | 0.621 |
| | Degree of fitting | 85.84% | 82.18% |
| | FPE | 0.038 | 0.022 |

response of the wire filler rate to the weld width $W_f$ under positive and negative step conditions are also not obvious. Under the condition of a positive step, the time-delay factor $d$ is close to 0 and less than that of a negative step, and the time constant $t$ is much greater than that of a negative step, indicating that an increase in wire filler metal leads to a sharp increase in arc thrust, which quickly affects weld formation. The gain coefficient $K$ of the weld width under a positive step condition of the wire filler rate is less than that under a negative step condition, which indicates that an increase in wire filler leads to the need for more heat for wire melting. It also shows that the welding current $I$ and wire filler rate $V_F$ play a decisive role in the shape characteristics of the weld pool, so it is correct to take the above two factors as the control variables of the hull structure GMAW.

After determining the time-delay factor of the two welding process parameters, the highest power of the nonlinear part is identified on the premise that the order of the linear dynamic subsystem is known. Taking the highest power $p_1^i, p_2^j$ $(i, j = 1, 2, \ldots)$ of the current and wire filling rate, a state that reduces the error index function, which tends to be smooth, can be obtained. The identification program is selected because the polynomial approximation theory of nonlinear systems (the essence of nonlinear characteristics is polynomial) proves that the greater the highest power $p$ is, the better the degree of accurate approximation. When $p$ is equal to the true power of the welding system, the error should be the smallest, and the error should remain unchanged theoretically when the value of $p$ increases. However, the highest power $p$ of the actual welding system is uncertain and may be very large, so a satisfactory error level can be obtained by increasing the linear order $m$.

Assuming that the order of the linear dynamic subsystem is known, $\{k = k_0+1, \cdots, k_0+N(N \geq l+p\times(m+1))\}$ is taken for formula (8) to obtain the least squares normal equation

$$\mathbb{Z} = \begin{bmatrix} \mathbb{Z}(k_0+1) \\ \vdots \\ \mathbb{Z}(k_0+N) \end{bmatrix} = \begin{bmatrix} \Gamma(k_0+1) \\ \vdots \\ \Gamma(k_0+N) \end{bmatrix} \cdot \vartheta = \aleph \cdot \vartheta \tag{10}$$

The final prediction error (FPE) criterion can be obtained

$$\Theta(\vartheta) = (\mathbb{Z} - \aleph\vartheta)^T(\mathbb{Z} - \aleph\vartheta) \tag{11}$$

The minimum value is taken to obtain the least squares solution as

$$\hat{\vartheta} = (\aleph^T\aleph)^{-1}\aleph^T\mathbb{Z} \tag{12}$$

where the model parameters correspond to

$$\begin{bmatrix} \hat{\alpha}_0, \cdots, \hat{\alpha}_N \\ \hat{\beta}_0, \cdots, \hat{\beta}_N \\ r_{i+1} \end{bmatrix} = \begin{bmatrix} \hat{\vartheta}(1), \cdots, \hat{\vartheta}(N) \\ \hat{\vartheta}(N+1), \cdots, \hat{\vartheta}(N+m+1) \\ \hat{\vartheta}(N+i(m+1)+l)/\hat{\vartheta}(l+N) \end{bmatrix}, \quad \begin{cases} i = 1, \cdots, p-1 \\ l = 1, \cdots, m+1 \end{cases} \tag{13}$$

With an increase in experimental data, the identification speed of the above algorithm will be slower, and too much old information will weaken the role of new information. Considering the real-time characteristics of the model structure, the recursive least squares (RLS) identification method is used to improve the performance.

Assuming the least squares normal equation $\mathbb{Z}_N = \aleph_N\vartheta$ where $N$ groups of observation data are measured, when the $N+1$ group of data $\mathbb{Z}(k_0+N+1)$ is measured, then

$$\aleph_{N+1} = \begin{bmatrix} \aleph_N \\ \aleph_{N+1} \end{bmatrix}, \quad \mathbb{Z}_{N+1} = \begin{bmatrix} \mathbb{Z}_N \\ \mathbb{Z}(k_0+N+1) \end{bmatrix} \tag{14}$$

Assuming $\Lambda_N = [\aleph_N^T\aleph_N]^{-1}$, the recursive formula can be obtained

$$\hat{\vartheta}_{N+1} = \hat{\vartheta}_N + \Lambda_N\aleph_{N+1}^T(1+\aleph_{N+1}\Lambda_N\aleph_{N+1}^T)^{-1} (\mathbb{Z}(k_0+N+1) - \aleph_{N+1}\hat{\vartheta}_N) \tag{15}$$

$$\Lambda_{N+1} = \Lambda_N - \Lambda_N\aleph_{N+1}^T(1+\aleph_{N+1}\Lambda_N\aleph_{N+1}^T)^{-1}\aleph_{N+1}\Lambda_N \tag{16}$$

The above formula can be simplified to

$$\begin{cases} \hat{\vartheta}_{N+1} = \hat{\vartheta}_N + K(N+1)(\mathbb{Z}(k_0+N+1) - \aleph_{N+1}\hat{\vartheta}_N) \\ K(N+1) = \Lambda_N\aleph_{N+1}^T(1+\aleph_{N+1}\Lambda_N\aleph_{N+1}^T)^{-1} \\ \Lambda_{N+1} = (E - K(N+1)\aleph_{N+1})\Lambda_N \end{cases} \tag{17}$$

The recursive initial value can be selected as

$$\begin{cases} \hat{\vartheta}_0 = 0 \\ \Lambda_0 = \ell^2 E = \begin{pmatrix} \ell^2 & \cdots & 0 \\ & \ddots & \\ 0 & \cdots & \ell^2 \end{pmatrix}, 10^5 \le \ell^2 \le 10^{10} \end{cases} \tag{18}$$

The FPE of the recursive algorithm is:

$$\max \left| \hat{\vartheta}_{N+1} - \hat{\vartheta}_N / \hat{\vartheta}_N \right| < \varepsilon \tag{19}$$

where $\varepsilon$ is appropriately small.

### D. EXCITATION SIGNAL TEST DESIGN FOR MODEL STRUCTURE IDENTIFICATION

The identification algorithm requires that the structural parameter $\aleph_N^T \aleph_N$ must be a regular matrix (reversible matrix), and the necessary and sufficient condition is that the input signal of the process parameters in the welding process must be a first-order continuous excitation signal. This means that the input required for structure identification cannot be selected arbitrarily; otherwise, the required identification effect cannot be achieved. At present, commonly used methods are random sequences (such as white noise), pseudo-random sequences, discrete series and so on. Combined with the dynamic process characteristics of ship GMAW, based on the advantages of no memory and no correlation with time of white noise, this example selects it to obtain the random excitation signal using the recursive congruence method.

The test platform required in this experiment is the robotic GMAW system, as shown in Figure 4. It mainly consists of a Kuka Arc5 robot, a pulsed GMAW power supply system, an industrial personal computer (IPC), a wire feeder, a visual sensing, a hall sensor, and a laser-based seam tracking system. The tracking system is used to identify the weld trajectory through laser scanning, guide the robot to move autonomously, and adjust the welding torch attitude to complete the welding preparation accurately and efficiently. The welding current and arc voltage are acquired by hall sensors. The visual sensing system is composed of a CCD camera, lenses, and special filters, by adjusting the relative position of the CCD camera and the workpiece, the geometric characteristics of the topside and backside weld pools can be obtained. The sampling frequency of the data acquisition card (DAQ) is set to 40 kHz, which can convert the collected analog signals into digital signals and send them to the data analysis module of the IPC. The processed feature information, such as welding current and wire filler rate, is input into the knowledge modelling module of industrial computer controller to obtain a posteriori probability prediction of weld formation, thus providing technical support for future research on welding quality control. Under reasonable welding specification parameters, the random variation range of the welding current and wire filler rate is determined. A robot welding test is carried out under the condition that the above two variables change randomly, and the shape parameters of the weld pool are extracted. The specific basic process conditions are shown in Table 3.

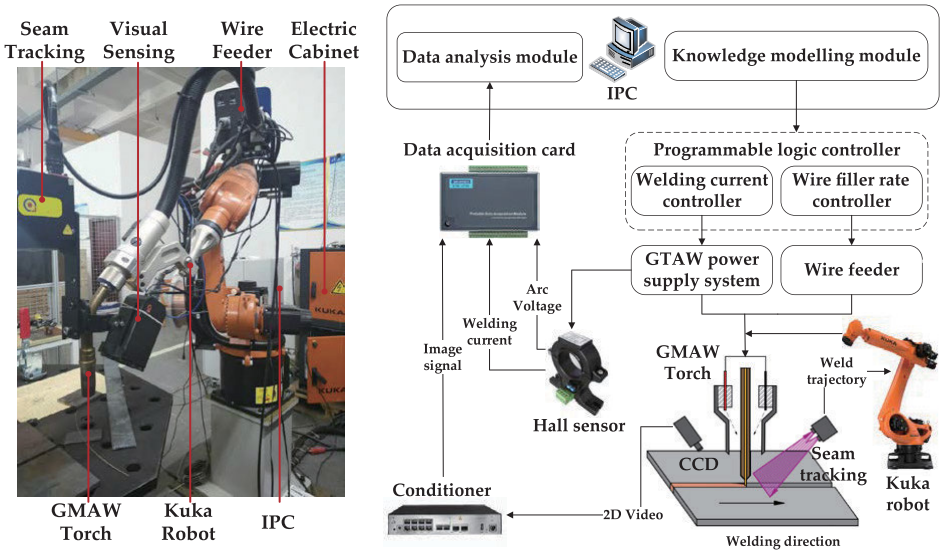


**FIGURE 4.** Physical and schematic diagram of the ship GMAW experimental platform.

**TABLE 3.** Random experimental conditions of ship hull GMAW.

| Factor Variables | Parameter Value | Factor Variables | Parameter Value |
|---|---|---|---|
| Structural material | Q235 | Specimen size | 300 × 150 × 8 (mm) |
| Welding wire diameter $\phi$ | 1.2 mm | Shielding gas | 80%Ar+20%$CO_2$ |
| Arc length $l$ | 2.0 mm | Gas flow $Q$ | 13 L/min |
| Welding current $I_p$ | 110–170 A | Wire filler rate $V_f$ | 2.3–4.7 m/min |
| Welding mode | MAG | Welding cone angle $\theta$ | 90° |
| Butt welding gap $\delta$ | 4.0 mm | Dry extension $\zeta$ | 15 mm |

### E. GMAW NONLINEAR MODEL OF THE HAMMERSTEIN STOCHASTIC NOISE

According to the Hammerstein model principle, the structure of the ship GMAW process knowledge model is complex. The characteristic output of the weld pool is related not only to the input of the welding process parameters at the current and some previous historical times but also to the stochastic system interference at a historical time. In this case, the characteristic size of the weld pool-front weld width $W_f$ is taken as the system output, and the system input is represented by the welding process parameters: welding current $I$ and wire filler rate $V_f$. The mathematical expression of the Hammerstein stochastic noise model [25] can be expressed as

$$\mathbb{Z}(k) = -\sum_{i=1}^{l} \alpha_i \mathbb{Z}(k-i) + \sum_{i_1=0}^{m_1} \sum_{j_1=1}^{p_1} \beta_{1i_1} \gamma_{1j_1} u_1^{j_1}(k - i_1 - d_1) + \sum_{i_2=0}^{m_2} \sum_{j_2=1}^{p_2} \beta_{2i_2} \gamma_{2j_2} u_2^{j_2}(k - i_2 - d_2) + e(k) \quad (20)$$

where $\mathbb{Z}$ represents the melting width $W_f$ of the system output; $u_1^{j_1}$ and $u_2^{j_2}$ represent the welding current and wire filler rate, respectively, of the system input; $e(k)$ is the stochastic white noise; $l$ is the linear order of the weld width at the historical time; $m_1$ and $m_2$ are the linear order of the welding current and wire filler rate, respectively; $p_1$ and $p_2$ are the nonlinear highest powers of the welding current and wire filler rate, respectively; and $d_1$ and $d_2$ are the time-delay factors of the welding current and wire filler rate of the nonlinear part, respectively.

Referring to the structural identification method of knowledge modelling for welding dynamic process, the structural parameters of the relationship model between weld width and welding current and wire filler rate are optimized. First, the time-delay factors $d_1$ and $d_2$ are determined according to the step response test. Second, on the basis of assuming the order $m_1$ and $m_2$ of the linear subsystem, the RLS method is used to increase the nonlinear power $p_1$ and $p_2$ to identify the optimal highest power value. Finally, the minimum loss function is found according to the FPE criterion and then the optimal order $m_1$ and $m_2$ of the linear subsystem is determined. See Figure 5 for the specific identification ideas.

Relying on the step response experimental results, the time-delay characteristics of the ship GMAW dynamic process are not obvious, and all the factors $d$ are less than 0.6. Therefore, the time-delay factors of the welding current and wire filler rate, which are input parameters to the GMAW nonlinear knowledge model, are set to 0. In this case, first, the particle filter algorithm is used to build the prediction model of forming characteristics, which follows the first-order Markov process, so it is concluded that the linear order $l$ of the weld width is set to 1. Second, depending on the principle of timeliness, the structural model should not be too complex. Assuming the linear order $m_1 = m_2 = 2$, the highest power of the optimal nonlinearity is determined as $p_1 = 1$, $p_2 = 3$ using the RLS method; see Figure 6 for details. Finally, the linear order is changed successively according to the optimal highest power, and the minimum loss function is found using the FPE criterion to determine the optimal linear order $m_1 = 1$, $m_2 = 3$, as shown in Figure 7.

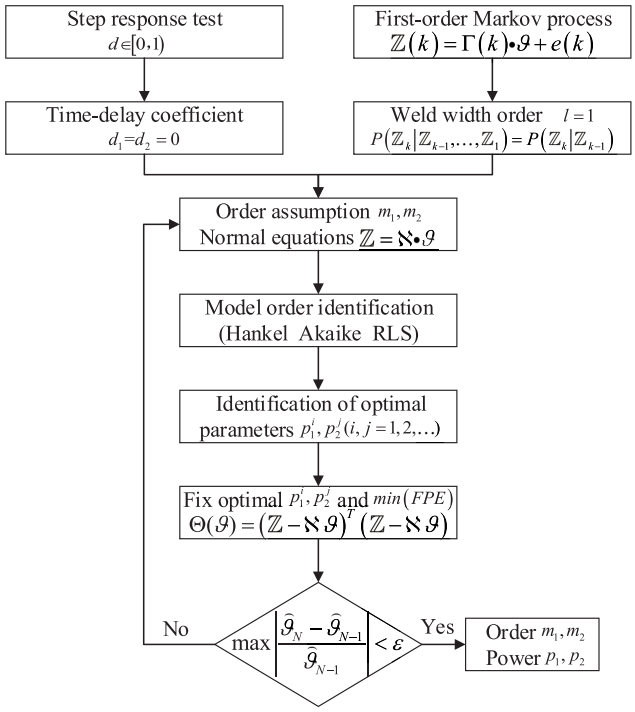


**FIGURE 5.** Structural identification of the GMAW nonlinear system model.

## III. DYNAMIC KNOWLEDGE MODELING METHOD OF SHIP GMAW

In the actual ship welding manufacturing process, weld observation sensor equipment is complex and has high installation requirements for hull structures. At the same time, the processing algorithm of image recognition and feature extraction is complex and time-consuming, which does not easily meet the target requirements of real-time observation and monitoring. Therefore, this paper uses the improved particle filter method to establish the GWMA dynamic knowledge model of hull structures to predict the weld characteristic information at the current time to provide accurate information feedback for the subsequent online real-time control of ship welding.

### A. PARTICLE FILTER

The particle filter in [30] is a Bayesian state estimation algorithm based on Monte Carlo simulation technology, which can deal with various forms of nonlinear and non-Gaussian problems. The core idea is to approximate the probability density function (PDF) by finding a group of stochastic samples propagating in the state space and replace the integral operation with the mean value of the samples to obtain the minimum variance distribution of the system state.

It is assumed that the welding nonlinear system can be defined as a dynamic state system model [31] composed of

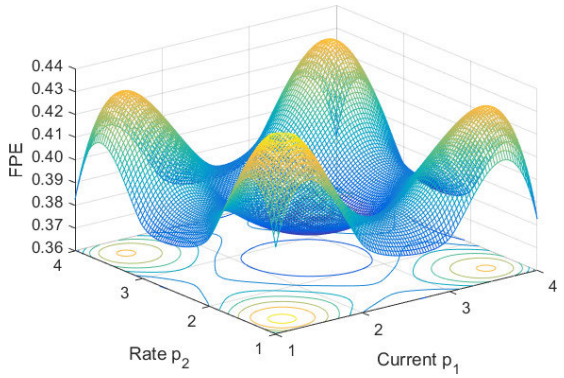


(a) Distribution curved surface diagram.

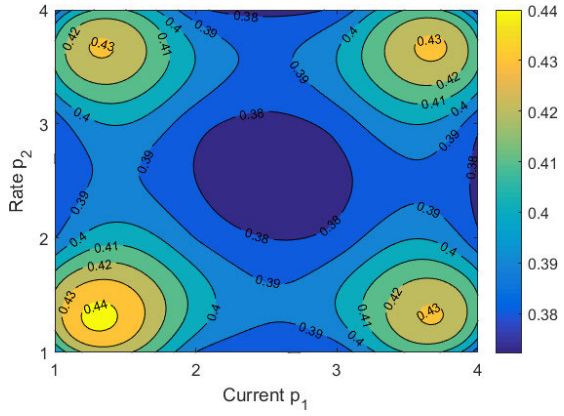


(b) Distribution cloud diagram.

**FIGURE 6.** Model structural identification of nonlinear highest power under the premise of fixed linear order.

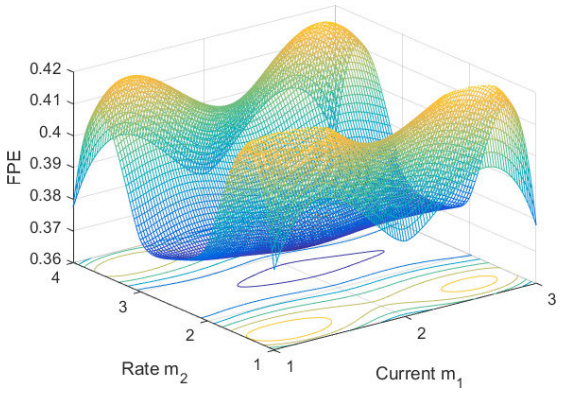


(a) Distribution curved surface diagram.

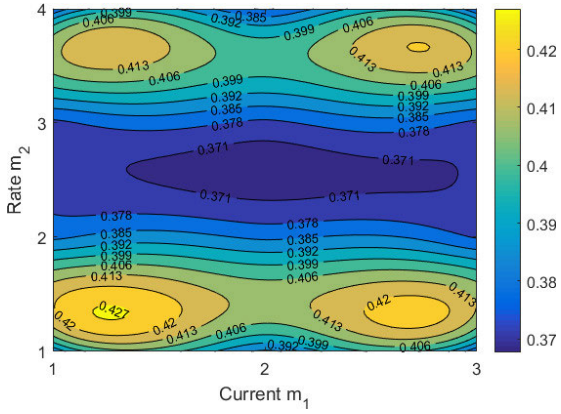


(b) Distribution cloud diagram.

**FIGURE 7.** Model structural identification of linear order under the premise of optimal highest power.

a group of time-varying and unobservable state sequences $x_k$ and a group of observation sequences $z_k$:

$$x_k = f(x_{k-1}, w_k) \quad \text{(State Transition)} \tag{21}$$
$$z_k = h(x_k, v_k) \quad \text{(Observation Equation)} \tag{22}$$

where $x_k$ and $z_k$ represent the system state and observation information at time $k$, $f(*)$ and $h(*)$ are the state transition and observation functions, and $w_k$ and $v_k$ are the system disturbance noise and observation noise at time $k$.

It is assumed that state $x_k$ follows a first-order Markov process, and $x_k$ remains independent of the observation information $z_k$. From the perspective of Bayesian theory, the problem of state estimation is to recursively calculate the reliability $p(x_k|z_{1:k})$ of the current state $x_k$ according to the existing observation data $z_{1:k}$ (a posteriori knowledge) at the previous time, which carries out the above recursion through two steps of prediction and update.

- Prediction

$x_{0:k} = \{x_i, i = 0, 1, \cdots, k\}$ represents the state variable from time 0 to $k$, and $z_{1:k} = \{z_1, z_2, \cdots, z_k\}$ represents the observation information corresponding to time 1 to $k$. Assuming that the PDF $p(x_{0:k-1}|z_{1:k-1})$ from time 0 to $k-1$ is known, the prior probability density function of state $k$ is calculated according to the Chapman-Kolmogorov theoretical formula:

$$\begin{aligned} p(x_{0:k}|z_{1:k-1}) &= \int p(x_k, x_{0:k-1}|z_{1:k-1})\mathrm{d}x_{0:k-1} \\ &= \int p(x_k|x_{0:k-1}, z_{1:k-1})p(x_{0:k-1}|z_{1:k-1})\mathrm{d}x_{0:k-1} \\ &= \int p(x_k|x_{0:k-1})p(x_{0:k-1}|z_{1:k-1})\mathrm{d}x_{0:k-1} \end{aligned} \tag{23}$$

- Update

The reliability of the state occurrence probability is estimated using the likelihood PDF $p(z_{1:k}|x_{0:k})$ of the observation information $z_{1:k}$ from time 0 to $k$. According to Bayesian theory, the posterior PDF $p(x_{0:k}|z_{1:k})$ of the state variable is estimated under the condition that the observation information marginal PDF $p(z_{1:k})$ and the state prior PDF $p(x_{0:k})$ are known:

$$\begin{aligned} &p(x_{0:k}|z_{1:k}) \\ &= \frac{p(z_{1:k}|x_{0:k}) \cdot p(x_{0:k})}{p(z_{1:k})} \\ &= \frac{p(z_k|x_{0:k}, z_{1:k-1}) \cdot p(x_{0:k}|z_{1:k-1})}{p(z_k|z_{1:k-1})} \\ &= \frac{p(z_k|x_{0:k}, z_{1:k-1}) \cdot p(x_k|x_{0:k-1}, z_{1:k-1}) \cdot p(x_{0:k-1}|z_{1:k-1})}{p(z_k|z_{1:k-1})} \\ &\propto p(z_k|x_k) \cdot p(x_k|x_{k-1}) \cdot p(x_{0:k-1}|z_{1:k-1}) \end{aligned} \tag{24}$$

The marginal PDF $p(z_{1:k})$ of the observation information can be transformed into a normalized constant:

$$p(z_{1:k}) = \int p(z_{1:k}|x_{0:k})p(x_{0:k})\mathrm{d}x_{0:k} \tag{25}$$

In the engineering application of nonlinear systems, due to the very complex operation of high-dimensional integrals, it is difficult to estimate the system state using two-step recursive operation. To solve the operation problem of the complex integral in the optimal Bayesian filtering algorithm, the Monte Carlo random sampling method [32] is introduced instead of calculating the a posteriori PDF $p(x_{0:k}|z_{1:k})$. The above basic idea can be understood as follows: when the problem required to be solved is the probability of an event or the expected value of a random variable, the occurrence probability is approximated by the frequency of the event or some statistical characteristics of the random variable are obtained as the problem solution, as can be found in Appendix A [33], [34].

However, after several iterations of *SIS* mentioned in the Appendix A, the importance weights of some particles may be as small as approximately negligible. This degradation phenomenon cannot be avoided due to the defects of the algorithm itself. Therefore, to reduce the influence of particle degradation, the importance resampling strategy is introduced. The essence of the strategy is to increase the diversity of particles and retain and copy the sample points with significant weight to adapt to the system dynamic process modelling to suppress the degradation phenomenon. Figure 8 shows the resampling process diagram of the particle filter algorithm. To measure the degradation degree of the importance weight and judge whether a resampling process is required, the following effective sampling scales $N_{eff}$ are calculated:

$$N_{eff} = \frac{1}{\sum_{i=1}^{N}(W_k^{(i)})^2} \tag{26}$$

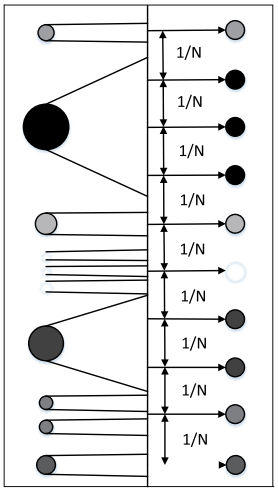


**FIGURE 8.** Process diagram of particle resampling in the PF algorithm.

The effective sampling scale $N_{eff}$ measures the degradation degree of particle importance weights. The larger the value, the greater the gap between particle weights, indicating that the more serious the weight degradation is. When it is greater than a certain threshold $N_{thre}$, n particle sets $x_k^{(i)*}$ are regenerated through a resampling strategy to meet the condition $x_k^{(i)} = x_k^{(i)*}$, and the weight $\hat{W}_k^{(i)} = 1/n$ of each new particle is given.

The posterior PDF of the sequential importance resampling (*SIR*) method, namely, the standard particle filter method, is calculated

$$p(x_{0:k}|z_{1:k}) \approx \sum_{i=1}^{n} \hat{W}_k^{(i)}(x_{0:k}^{(i)})\delta(x_{0:k} - x_{0:k}^{(i)}) \tag{27}$$

### B. CLUSTERING SIMILARITY PARTICLE FILTER

In the *SIS* process of the standard PF algorithm, since the prior PDF is assumed to be a known proposed distribution, the particle weight variance will continue to accumulate with the increase in the number of iterations, and the weight corresponding to most particles will be reduced to a negligible degree, which is the phenomenon of particle degradation [35]. Degradation means that continuous iterative operation causes many computing resources to be consumed on insignificant particles with small weight, resulting in excessive waste of computing time. At the same time, state estimation cannot accurately express the real posterior distribution. Aiming at the problem of particle degradation, a resampling strategy is introduced to increase the diversity of particles, which also causes new problems: particles with large weights are selected for sampling many times, while particles with low weights are discarded, which makes the sampling results contain more repeated particles and cannot effectively and truly reflect the probability distribution of the state variables, resulting in the problem of sample depletion [36]. Thus, the state estimation variance becomes larger, and the filtering performance is greatly reduced. Therefore, to solve the two defects of the particle filter algorithm itself, a clustering similarity particle filter algorithm based on the principle of state trajectory consistency [37] is proposed in this paper. Based on an information fusion model of the spatial state trajectory, this method uses data mining analysis to measure the clustering similarity of current and future multistage observation information to perfect the proposed distribution, guide the importance sampling process to effectively improve the phenomenon of particle degradation, and abandon the resampling strategy to solve the problem of particle depletion. Appendix B provides further details of specific formula deduction for CSPF [38].

Based on the above theory, the improved algorithm process is as follows:

$$\begin{Bmatrix} k \\ k+L+l \end{Bmatrix} \mapsto \begin{Bmatrix} x_k^{\circ}(i) \\ x'_{k+L+l}(i) \end{Bmatrix} \sim \begin{Bmatrix} \mathrm{SIS} \\ \mathrm{GPF} \end{Bmatrix} \Rightarrow \begin{Bmatrix} W_k^{\bullet}(i) \\ W_{k+L+l}^{\bullet}(i) \end{Bmatrix} \tag{28}$$

Among them, the particle distribution $\{x_k^{\circ}(i)\}_{i=1}^{n}$ sampled by the *SIS* filter at time $k$ and its corresponding importance weight $\{W_k^{\bullet}(i)\}_{i=1}^{n}$ can approximately represent the state

estimation of the posterior PDF $p(x_k|z_{1:k})$, and the particle distribution $\{x'_{k+L+l}(i)\}_{i=1}^n$ sampled by the *GPF* prediction at time $k+L+l$ and its corresponding importance weight $\{x'_{k+L+l}(i)\}_{i=1}^n$ can approximately represent the state prediction of prior PDF $p(x_{k+L+l}|z_{1:k})$. Therefore, the current time state estimation $x_k$ can be obtained using a filtering operation, and the future time state prediction $x_{k+L+l}$ can be obtained using a prediction step. The specific implementation of the improved algorithm is as follows:

- Recursive prediction

The step is consistent with the *SIS* filtering and *GPF* prediction process, and sampling forms particle set $\{X_k^\bullet(i)\}_{i=1}^n$;

- Update correction

The *SIS* model is modified and updated using the observation similarity between the current filter (original trajectory) and the future multistage Gaussian prediction (modified trajectory) [39], and then the corresponding importance weights $\{W_k^\bullet(i)\}_{i=1}^n$ and $\{W_{k+L+l}^\bullet(i)\}_{i=1}^n$ are calculated and normalized to obtain $\{W_k(i)\}_{i=1}^n$ and $\{W_{k+L+l}(i)\}_{i=1}^n$.

$$x_k \approx \tilde{x}_k = \sum_{i=1}^{n} W_k(i) x_k^\bullet(i) \quad \text{(Filtering)} \tag{29}$$

$$x_{k+L+l} \approx \tilde{x}_{k+L+l} = \sum_{i=1}^{n} W_{k+L+l}(i) x'_{k+L+l}(i) \quad \text{(Prediction)} \tag{30}$$

The above steps constitute an iterative process of the improved algorithm. Different from the standard PF, the method consists of prediction(filtering)-update-filtering (prediction) without resampling steps. The specific algorithm steps are shown in Algorithm 1.

**Algorithm 1** Clustering Similarity Particle Filter

Step 1 Particle set initialization
For $i = 1, 2, \cdots, n$, at time $k = 0$
Sample initial particle set $\{x_0\}_{i=1}^n$ by prior PDF
$x_0^{(i)} \sim p(x_0)$, $W_0^{(i)} = 1/n$
For $i = 1, 2, \cdots, n$, at time $k \geq 1$
Step 2 Importance sampling process
Select importance PDF $\pi(x_{0:k}|z_{1:k})$
Predict prior PDF $p(x_{0:k}|z_{1:k-1})$ at time $k$
$x_k^{(i)} \sim \pi(x_k|x_{0:k-1}^{(i)}, z_{1:k})$
Step 3 Calculate similarity measurement
Compose state trajectories $\{X_k^\bullet(i)\}_{i=1}^n$
Draw $x_j^\circ(i) \sim SIS, j = k, \cdots, k+L$
$x'_j(i) \sim GPF, j = k+L+1, \cdots, k+L+l$
Evaluate observation likelihood trajectories
$Z_k^\bullet(i) = h(X_k^\bullet(i), v_k)$
Calculate distance similarity measurement
$D_k^\bullet(i) = dis(\{Y_k\}, \{Y_k^\bullet(i)\}_{i=1}^n)$
Exponential transformation
$D_k(i) = e^{\lambda \times D_k^\bullet(i)}$
Step 4 Update importance weights
Modified proposal distribution
$\pi(x_k|x_{k-1}^{(i)}, z_k) = D_k(i) p(x_k|x_{k-1}^{(i)})$
Recursive weights
$W_k^\bullet(i) \propto D_k^{-1}(i) p(z_k|x_k^{(i)})$
$W_{k+L+l}^\bullet(i) \propto D_k^{-1}(i) p(z_{k+L+l}|x_{k+L+l}^{(i)})$
And normalize
$W_k(i) = \frac{W_k^\bullet(i)}{\sum_{i=1}^n W_k^\bullet(i)}$
$W_{k+L+l}(i) = \frac{W_{k+L+l}^\bullet(i)}{\sum_{i=1}^n W_{k+L+l}^\bullet(i)}$
Step 5 Bayesian state estimation
$x_k = \sum_{i=1}^n W_k(i) x_k^{(i)}$
$x_{k+L+l} = \sum_{i=1}^n W_{k+L+l}(i) x_{k+L+l}^{(i)}$
Let $k = k+1$ and repeat Steps 2–5 in sequence.

### C. CONVERGENCE OF THE CSPF

The clustering similarity particle filter fully conforms to the principle of the Bayesian state estimation method in boost filtering theory, which is realized by weighted bootstrapping [34], [40]. It is assumed that the combined set $\{X_k^\bullet(i)\}_{i=1}^n$ of the state trajectory obeys the continuous PDF $G(x)$, the posterior probability distribution obtained by the CSPF algorithm has a constant coefficient proportional relationship with $G(x)U(x)$, and $U(x)$ is a known corresponding weight function. In this case, referring to formula (42), it can be seen that the state posterior PDF $p(x_k|z_{1:k})$ has a constant proportional relationship with the product of the observation likelihood PDF $p(z_k|x_k)$ and the prior PDF $p(x_k|z_{1:k-1})$, in which $G(x)$ can be regarded as the state prior PDF $p(x_k|z_{1:k-1})$, and referring to formula (54), the weight $U(x)$ can be equivalent to the product of the observation likelihood function $p(z_k|x_k)$ and the clustering similarity measure. Then, when the number of samples is $n \to \infty$, the particle discrete distribution composed of trajectory set $\{X_k^\bullet(i)\}_{i=1}^n$ and corresponding normalized weight $\{U(X_k^\bullet(i))/\sum_{i=1}^n U(X_k^\bullet(i))\}_{i=1}^n$ can approach the posterior probability density distribution of the actual system. Clearly, the improved method conforms to boost filtering theory, and the results are reasonable and effective.

*Remark 3.1:* In the CSPF algorithm, the prior probability density of importance sampling is consistent with the transfer density function used in the *SIS* process. $n \times (L+l)$ particles are sampled according to *SIS* filtering and *GPF* prediction and then combined into a particle set of state trajectories.

*Remark 3.2:* The difference between the CSPF algorithm and the standard PF is that the state trajectory similarity is used to guide the generation of the new proposed distribution, the sampled particles close to the actual state are selected to increase their weight to improve the particle degradation phenomenon, and the state trajectory is represented by the observation likelihood trajectory instead.

*Remark 3.3:* In the CSPF algorithm, the first-order Markov process is updated to compensate and modify the sequential importance weight to replace the resampling strategy and eliminate the particle depletion problem, which not only reduces the complexity of the algorithm but also does

not reduce the effectiveness of the accuracy of the prediction results.

*Definition 3.1:* The system state $X$ follows a first-order Markov process, that is, the state $X_k$ at the current time is only related to the state $X_{k-1}$ at the previous time. Assuming the initial state $X_0(i) \sim p(x_0)$, the state transition kernel function $K(x_k|x_{k-1})$ and the observation likelihood PDF $B(z_k|x_k)$ can be expressed as Lebesgue measures, which can be obtained by referring to formulas (21) and (22).

$$K(x_k|x_{k-1}) = p_w(x_k - f(x_k)) \tag{31}$$

$$B(z_k|x_k) = p_v(z_k - h(x_k)) \tag{32}$$

where $p_w$ and $p_v$ are the probability density distributions under the influence of state process noise $w_k$ and observation noise $v_k$, respectively.

*Theorem 3.1:* It is assumed that the state transition kernel density function $K$ satisfies the first-order Markov process, and the observation likelihood probability density function $B$ is continuous, bounded and strictly positive in the range of $x_k \in \Re^{n_x}$. Under the random disturbance $c^n$ influence of Monte Carlo sampling, the state estimation measure $\hat{\varpi}^n_{k|k}$ of the CSPF algorithm converges to the theoretical state measure $\varpi_{k|k}$ of the Bayesian optimal filter (actual system state):

$$\lim_{n\to\infty} \hat{\varpi}^n_{k|k} = \varpi_{k|k} \tag{33}$$

The proof process of Theorem 3.1 is referred to Appendix C [41], [42], [43].

## IV. STATE TRACKING AND WELD FORMING PREDICTION OF SHIP GMAW DYNAMIC PROCESS

Weld width, reinforcement and welding penetration are important indexes to evaluate the forming quality, while welding penetration and reinforcement are difficult to obtain in real time during the welding dynamic process. Therefore, in this case, the weld width is selected as the main factor of welding reliability. Ship GMAW is a complex process with time-varying, multivariable, coupling, and strong nonlinearity. To obtain a mathematical model between the welding specification parameters and weld width, it is necessary to establish a weld width prediction model according to relevant artificial intelligence methods. Existing theories and application cases have proven the advantages of particle filter technology in nonlinear and non-Gaussian systems, but this method still has the problems of particle degradation caused by an unknown importance probability density function and particle depletion caused by resampling strategy. Therefore, in this example, the particle filter method is adopted to establish a dynamic knowledge model of ship GMAW process under the combined influence of nonlinear welding mechanism and stochastic interference noise, which can substitute for the previous modelling method with more subjective factors relying on a lot of prior knowledge, expert experience and hardware detection technology. Furthermore, the advantages of particle filter in deep data mining are fully utilized to reveal the objective change rule and the temporal dynamic relationship of welding process parameters and weld formation. This results in ensuring the accuracy of output response even under input conditions with fewer types of parameters, and significantly reduces the hardware requirements of GMAW platform sensing and the computational cost of knowledge model. Meanwhile, the cluster analysis method is used to measure the distance similarity between the trajectory state set of the actual system and the sampled particles, guide the generation of a new proposed distribution and update the importance sampling process to reduce the impact of particle degradation and abandon the resampling strategy to solve the problem of particle depletion. On the premise of making full use of the advantages of particle filter in nonlinear applications, it is improved to enhance the accuracy and timeliness of state tracking and forming prediction in welding dynamic process.

Based on this, this paper takes the model architecture of Hammerstein random noise as the core and uses the CSPF algorithm to establish an estimation model of state tracking and forming prediction for the dynamic process of ship welding. First, a structural identification model is created for the historical samples of the ship welding process, a reasonable identification test is designed, and an efficient and practical fitting algorithm is selected to identify and optimize the structural parameters, which is convenient for building a state space model (state transition and observation equation) to provide a theoretical basis for welding forming prediction. Second, the cluster analysis method is used to measure the distance similarity between the observation trajectory information predicted by the current stage filter (original trajectory) and the future multistage Gaussian filter (modified trajectory), which is used to modify the importance PDF to update the weight calculation in the importance sampling process to improve the particle degradation phenomenon. Finally, the Bayesian method is used to train the state tracking and parameter optimization of the space model, and then the prediction knowledge model of ship GMAW forming based on the CSPF is constructed. At the same time, the simulation schemes of different knowledge models are designed to verify the reliability characteristics such as the prediction accuracy and timeliness of the improved method. Figure 9 shows the state tracking and forming prediction method for the ship welding dynamic process.

According to the state tracking training and parameter identification method of the GMAW dynamic process, several groups of data under the experimental process conditions in Table 3 are selected as the original data set $OX$ of the welding test. The standard particle filter (PF), auxiliary particle filter (APF) and CSPF algorithm are used for simulation and comparison. $OS$ is selected as the training set of state tracking, and $SX$ is selected as the test set of forming prediction. Among all algorithms, the state space equation is initialized by the Hammerstein stochastic noise model after structure identification (refer to formula (20) and Figure 5) and the historical data set $OS$, in which the number of tracking steps $k = 1, 2, \ldots, S$ and $S = 120$, the number of sampling particles $N = 200$, the number of running simulations

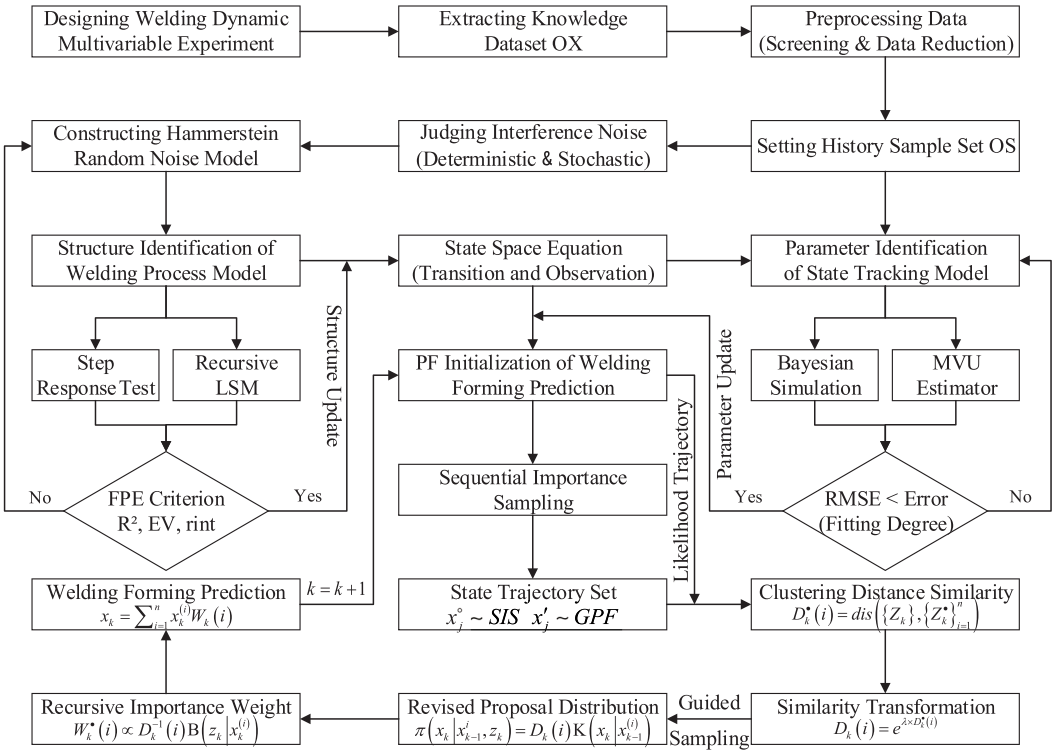


**FIGURE 9.** State tracking and forming prediction method for the ship welding dynamic process.

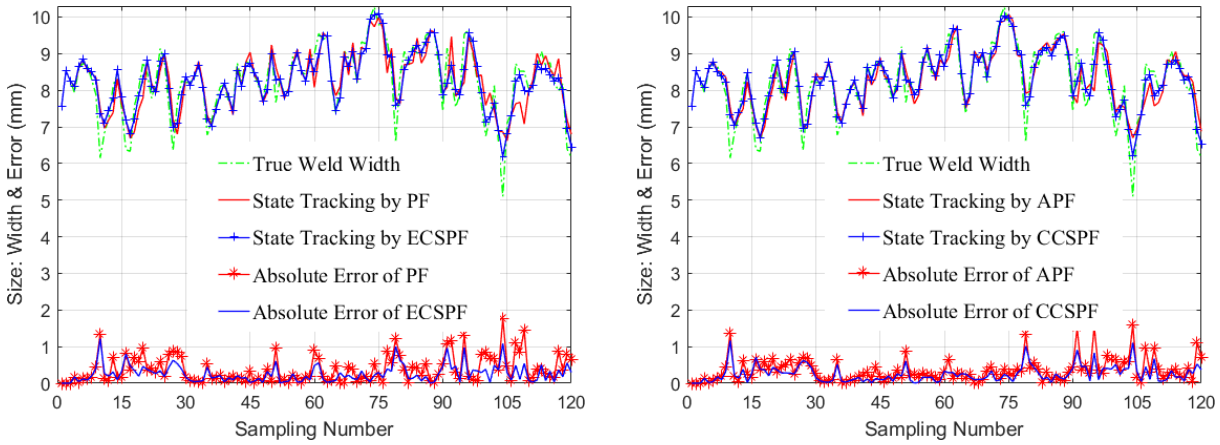


(a) PF and ECSPF. (b) APF and CCSPF.

**FIGURE 10.** State tracking for the ship welding dynamic process based on four nonlinear prediction models.

$T = 200$, the state initial value $x_1 = \{OS\}_{k=1}$, the residual resampling strategy $RS = RR$, the noise of state tracking is $v_k \sim N(0, R_k^2)$ and $R_k^2 = 1$, the number of prediction steps $k = S, S+1, \ldots, X$ and $X = 200$, the noise of forming prediction is $w_k \sim N(0, Q_k^2)$ and $Q_k^2 = 0.1$ are selected. The computer processor speed is 3.40 GHz, and the RAM is 16.0 GB. The absolute error (AE) and root mean square error (RMSE) are selected as the evaluation factors of the state tracking effect and forming prediction accuracy of various algorithms. $x^{tur}$ and $x^{est}$ represent the test true value and state estimation value, respectively, i.e.,

$$AE = |x_k^{tur} - x_k^{est}| \tag{34}$$

$$RMSE = \sqrt{\frac{1}{S}\sum_{k=1}^{S}(x_k^{tur} - x_k^{est})^2} \tag{35}$$

In addition, in the CSPF algorithm, the correlation coefficients $L = 2$ and $l = 1$, the reliable gradient factor $\lambda = -1$, the clustering similarity adopts two similarity measures of spatial distance, in which CCSPF represents the similarity

**TABLE 4. Average effect comparison of the state tracking for nonlinear prediction models running 200 times.**

| Filter | SSE | MSE | RMSE | R-squared |
|---|---|---|---|---|
| PF | $1.679 \times 10^{-1}$ | $1.4 \times 10^{-3}$ | $2.7 \times 10^{-3}$ | $6.722 \times 10^{-1}$ |
| APF | $1.389 \times 10^{-1}$ | $1.2 \times 10^{-3}$ | $2.4 \times 10^{-3}$ | $7.120 \times 10^{-1}$ |
| ECSPF | $0.753 \times 10^{-1}$ | $6.5 \times 10^{-4}$ | $1.8 \times 10^{-3}$ | $8.510 \times 10^{-1}$ |
| CCSPF | $0.708 \times 10^{-1}$ | $6.1 \times 10^{-4}$ | $1.7 \times 10^{-3}$ | $8.519 \times 10^{-1}$ |

**TABLE 5. Average effect comparison of the forming prediction for four prediction models running 200 times.**

| Comparison Item | PF | APF | CSPF | |
|---|---|---|---|---|
| | | | ECSPF | CCSPF |
| RMSE Mean | $8.804 \times 10^{-1}$ | $8.439 \times 10^{-1}$ | $4.801 \times 10^{-1}$ | $4.731 \times 10^{-1}$ |
| RMSE Variance | $7.0 \times 10^{-3}$ | $6.4 \times 10^{-3}$ | $2.6 \times 10^{-5}$ | $2.5 \times 10^{-5}$ |

Note: RMSE Mean = the mean of the RMSE, RMSE Variance = the variance of the RMSE.

algorithm of Chebyshev spatial distance (measurement type parameter $\kappa = \infty$), and ECSPF represents the similarity algorithm of Euclidean spatial distance (measurement type parameter $\kappa = 2$). Figures 10–12 and Tables 4–5 show the comparison effect of various algorithms between the training effect of state tracking and the results accuracy of forming prediction, in which the table results are quantitatively compared by running 200 simulation calculations. Among them, the effect indicators of the state tracking include the absolute error (AE), sum of squares due to error (SSE), mean square error (MSE), root mean square error (RMSE) and R-squared (coefficient of determination); the closer AE, SSE, MSE and RMSE are to 0 and the closer R-squared is to 1, the better the performance of state tracking. The accuracy indicators of forming prediction include the AE, RMSE mean and RMSE variance.

Figure 10 shows that the state tracking effects of the four methods are good. They are relatively consistent with the actual change trend of weld formation under different welding process conditions, accurately extract the forming change trend implied in the state part of the tracking set $OS$, and provide accuracy assurance for maintaining the same welding law of the forming prediction in the test set $SX$. Combined with Table 4, the effect indicators of the CSPF state tracking are obviously dominant. Taking ECSPF as an example, the SSE is increased by 55% and 46% compared with the PF and APF, the MSE is increased by 54% and 46%, the RMSE is

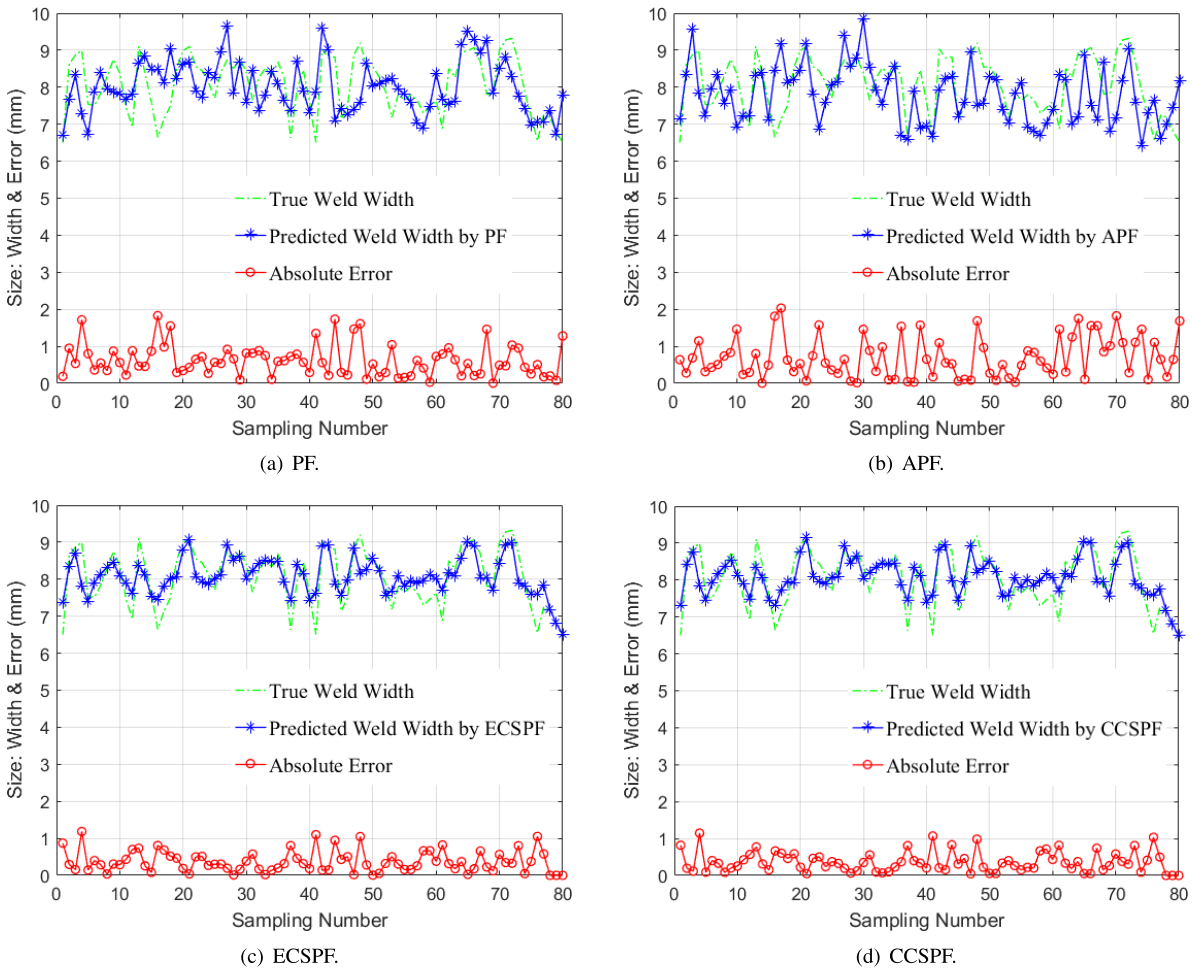


(a) PF. (b) APF. (c) ECSPF. (d) CCSPF.

**FIGURE 11. Forming prediction for the ship welding dynamic process based on four nonlinear prediction models.**

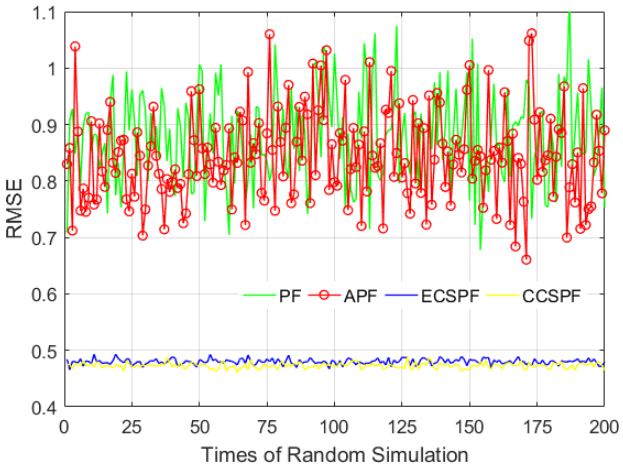


**FIGURE 12.** RMSE comparison of the forming prediction based on four prediction models running 200 times.

increased by 33% and 25%, and R-squared is increased by 27% and 20%, respectively. It can also be seen that CCSPF state tracking has the best training effect and strong stability.

Figure 11 shows the comparison of forming results and absolute error between different nonlinear prediction models and the actual weld state. Combined with Table 5, it can be seen that the prediction trend of the four methods is basically consistent with the actual state of the test set *SX*, and the RMSE mean of the prediction results is maintained below 0.88 mm, which shows that the particle filter methods have certain suitability in the application of knowledge modelling such as state tracking and forming prediction in the dynamic process of hull structure GMAW. Figure 12 demonstrates the RMSE comparison of forming prediction for different nonlinear models running 200 simulations randomly, compared with the PF and APF methods, the prediction trend of the CSPF is closer to the characteristic curve of welding forming, and the AE, RMSE and RMSE mean (variance) of the prediction results are greatly reduced. Taking CCSPF method as an example, the RMSE mean of the forming prediction is reduced by 46% and 44%, respectively, indicating that the forming prediction accuracy of the CSPF method is higher. The curve of the RMSE mean is relatively stable, and its variance is reduced by approximately 280 times and 260 times, respectively, which indicates that the dispersion degree of the particle set representing the state of the CSPF forming prediction result is the smallest, the expression degree of uncertainty is the lowest, and the robust stability is stronger.

Under the condition of setting the same running time, the state estimation accuracy of forming prediction is obtained by adjusting the number of sampling particles, and the operation efficiency of various algorithms is proved by comparing the corresponding running cost; see Table 6 for details. It can be seen from Table 6 that under the premise of the same operation cost, the number of sampling particles used by the CSPF algorithm is the lowest, and the accuracy indicators of forming prediction are significantly higher than those of

**TABLE 6.** Comparing analysis for four prediction models running 200 times under the same running time.

| Filter | N | RMSE Mean | RMSE Variance | AVG Time (s) |
|---|---|---|---|---|
| PF | 550 | $8.554 \times 10^{-1}$ | $6.4 \times 10^{-3}$ | 0.1 |
| APF | 270 | $8.381 \times 10^{-1}$ | $6.1 \times 10^{-3}$ | 0.1 |
| ECSPF | 200 | $4.801 \times 10^{-1}$ | $2.6 \times 10^{-5}$ | 0.1 |
| CCSPF | 200 | $4.731 \times 10^{-1}$ | $2.5 \times 10^{-5}$ | 0.1 |

Note: N = the number of particles sampled, RMSE Mean = the mean of RMSE, RMSE Variance = the variance of RMSE, AVG = average.

the PF and APF, in which the RMSE mean is approximately twice as high. Therefore, it is verified that the CSPF algorithm has higher operation efficiency and outstanding timeliness advantages.

## V. CONCLUSION

The clustering similarity particle filter (CSPF) method based on state trajectory consistency is proposed to solve the knowledge modelling problem of the ship hull structure GMAW process with strong nonlinear characteristics. *SIS* filtering and *GPF* prediction are used to obtain the current and future multistage state information to form a spatial combination trajectory, and the clustering principle is selected to measure the trajectory similarity between the spatial combination and the actual state to guide the generation of a new proposed distribution to reduce the impact of particle degradation. Then, the importance weight calculation is updated with the latest observation information to replace the resampling strategy to finally eliminate the particle depletion problem. Meanwhile, a convergence theorem for the CSPF method is proposed and proved theoretically. A step response test is designed, and the recursive least squares method is selected to identify the structure of the Hammerstein model representing the welding process of stochastic noise interference. Then, the GMAW knowledge model of state tracking training and weld forming prediction based on the CSPF method is established. Application cases and experiments show that compared with the standard PF and APF, the CSPF model has significant advantages in accuracy, robustness and efficiency in the training effect of state tracking and the prediction results of weld forming. The main conclusions are summarized as follows:

1) The training effect of state tracking based on the PF, APF and CSPF is good to ensure that the forming trend and influence mechanism impliedin the training set can be accurately extracted; the prediction trend of weld formation is consistent with the actual change curve of the test set, and the accuracy is maintained within 0.88 mm, which shows that the particle filter method has certain adaptability in the application of GMAW dynamic knowledge modelling.

2) The CSPF model adopts the cluster similarity of the state trajectory to compensate for the importance sampling process affected by an unreasonable proposed distribution, which makes the effect indicators of state tracking better and provides an accuracy guarantee for the forming prediction of the weld model. Compared with the PF and APF, the RMSE mean of the CSPF prediction is reduced by approximately 45%,

and the variance is reduced by approximately 270 times, which shows that the CSPF model has higher prediction accuracy, a lower degree of uncertainty expression and stronger robust stability.

3) The CSPF model ensures computational efficiency by reducing the number of sampling particles and the order of state trajectory. In the same calculation time, the number of sampling particles used by the CSPF method is relatively minimal on the premise of selecting a reasonable trajectory order, while the prediction accuracy of weld formation is much higher than that of the PF and APF, which is approximately twice as high, indicating that the CSPF method has higher operation efficiency.

The Hammerstein stochastic noise model, which is more conforming to the weld forming rule, abstracts from the dynamic welding process and provides theoretical support for knowledge modelling. Meanwhile, the improved particle filter method ensures the prediction precision of ship GMAW forming. Besides, the limited experimental conditions may not fully represent the actual production environment. Nevertheless, we provide a new method to predict welding quality, it is concluded that particle filter has good application prospects in welding quality monitoring. In future, more adequate welding tests will be carried out in factory to find out unknown types of interference effects, some effort will be done to refine noise model with more objective factors to achieve more accurate expression of weld forming mechanism.

## APPENDIX

### A. SEQUENTIAL IMPORTANCE SAMPLING (SIS)

Assuming that $n$ independent identically distributed (i.i.d.) samples $\{x^{(i)}, i = 1, 2, \cdots, n\}$ $(n \geq 1)$ can be sampled from the posterior PDF $p(x_k|z_{1:k})$, the approximate estimation of the posterior PDF can be expressed as:

$$\hat{p}(x_k|z_{1:k}) = \frac{1}{n}\sum_{i=1}^{n}\delta\left(x_k - x_k^{(i)}\right) \approx p(x_k|z_{1:k}) \tag{36}$$

where $\delta(x)$ is the Dirac function. The Monte Carlo method is used to directly estimate the expected value of the a posteriori PDF:

$$\begin{aligned}\hat{E}[f(x_k)] &\approx \int f(x_k)\hat{p}(x_k|z_{1:k})\mathrm{d}x_k \\ &= \frac{1}{n}\sum_{i=1}^{n}\int f(x_k)\delta(x_k - x_k^{(i)})\mathrm{d}x_k = \frac{1}{n}\sum_{i=1}^{n} f(x_k^{(i)})\end{aligned} \tag{37}$$

It can be obtained according to the strong law of large numbers [33]

$$\lim_{n\to\infty}\hat{E}_{\hat{p}(x_k|z_{1:k})}[f(x)] \underset{\text{a.s.}}{\longrightarrow} E_{p(x_k|z_{1:k})}[f(x)] \tag{38}$$

According to the central limit theorem [33], the convergence rate is expressed as

$$\sqrt{n}(\hat{E}_{\hat{p}(x_k|z_{1:k})}[f(x)] - E_{p(x_k|z_{1:k})}[f(x)]) \sim N(0, \sigma_f^2) \tag{39}$$

where $\sigma_f^2$ is the variance of $f(x)$. It can be concluded that the error order $O(N^{1/2})$ of the Monte Carlo method is independent of the integral dimension and is suitable for solving high-dimensional complex integrals. However, the posterior PDF $p(x_k|z_{1:k})$ does not always produce an analytical formula, which makes it difficult to extract samples from the distribution directly. Therefore, it is necessary to introduce the sequential importance sampling (*SIS*) [34] method to solve the sampling problem.

It is assumed that the i.i.d. particle sets $\{x^{(i)}, i = 1, 2, \cdots, n|n \geq 1\}$ are extracted from known importance PDF $\pi(x_{0:k}|z_{1:k})$. When the number of particles $n \to \infty$, the importance PDF $\pi(x_{0:k}|z_{1:k})$ is highly similar to the a posteriori PDF $p(x_{0:k}|z_{1:k})$, which can be decomposed into recursive form

$$\pi(x_{0:k}|z_{1:k}) = \pi(x_{0:k-1}|z_{1:k-1})\pi(x_k|x_{0:k-1}, z_{1:k}) \tag{40}$$

The importance PDF $\pi(x_{0:k}|z_{1:k})$ is introduced to solve the Monte Carlo high-dimensional complex integral problem:

$$\begin{aligned}E[f(x_{0:k})] &= \int f(x_{0:k})\frac{p(x_{0:k}|z_{1:k})}{\pi(x_{0:k}|z_{1:k})}\pi(x_{0:k}|z_{1:k})\mathrm{d}x_{0:k} \\ &= \int f(x_{0:k})W_k^{(i)}(x_{0:k})\pi(x_{0:k}|z_{1:k})\mathrm{d}x_{0:k}\end{aligned} \tag{41}$$

In the importance sampling process, the state $x_{k-1}$ at time $k-1$ is updated through the particle $x_k^{(i)}$ at time $k$:

$$p(x_{0:k}|z_{1:k}) = p(x_0)\prod_{i=1}^{k}\frac{p(y_i|x_i)p(x_i|x_{i-1})}{p(z_i|z_{i-1})} \tag{42}$$

The importance weight $W_k^{(i)}(x_{0:k})$ of time $k$ can be obtained

$$\begin{aligned}W_k^{(i)}(x_{0:k}) &= \frac{p(x_{0:k}|z_{1:k})}{\pi(x_{0:k}|z_{1:k})} \\ &= \frac{p(x_0)}{\pi(x_0)}\prod_{i=1}^{k}\frac{p(z_i|x_i)p(x_i|x_{i-1})}{p(z_i|z_{1:i-1})\pi(x_i|x_{0:i-1}, z_{1:i})}\end{aligned} \tag{43}$$

The importance PDF $\pi(x_{0:k}|z_{1:k})$ can be decomposed into

$$\pi(x_{0:k}|z_{1:k}) = \pi(x_0)\prod_{i=1}^{k}\pi(x_i|x_{0:i-1}, z_{1:i}) \tag{44}$$

In the actual calculation process, the particle set $x_k^{(i)}$ can be sampled and obtained according to the following formula:

$$x_k^{(i)} \sim \pi(x_k|x_{0:k-1}^{(i)}, z_{1:k}) \tag{45}$$

The recursive importance weight $\tilde{W}_k^{(i)}$ is

$$\tilde{W}_k^{(i)} \propto \tilde{W}_{k-1}^{(i)}\frac{p(z_k|x_k^{(i)})p(x_k^{(i)}|x_{k-1}^{(i)})}{\pi(x_k^{(i)}|x_{0:k-1}^{(i)}, z_{1:k})} \tag{46}$$

In sequential importance sampling, it is assumed that the importance distribution $\pi(x_k|x_{0:k-1}^{(i)}, z_{1:k})$ satisfies:

$$\pi(x_k|x_{0:k-1}^{(i)}, z_{1:k}) \sim \pi(x_k|x_{k-1}^{(i)}, z_k) \tag{47}$$

The recursive sequential importance sampling weight is

$$\tilde{W}_k^{(i)} \propto \tilde{W}_{k-1}^{(i)} \frac{p(z_k|x_k^{(i)})p(x_k^{(i)}|x_{k-1}^{(i)})}{\pi(x_k^{(i)}|x_{k-1}^{(i)}, z_k)} \tag{48}$$

Normalizing the recursive importance weight $W_k^{(i)}$

$$W_k^{(i)} = \frac{\tilde{W}_k^{(i)}}{\sum_{i=1}^n \tilde{W}_k^{(i)}} \tag{49}$$

Finally, the posterior PDF of *SIS* is calculated, i.e.,

$$p(x_{0:k}|z_{1:k}) \approx \sum_{i=1}^{n} W_k^{(i)}(x_{0:k}^{(i)})\delta(x_{0:k} - x_{0:k}^{(i)}) \tag{50}$$

where $\tilde{W}_k^{(i)}(x_{0:k}^{(i)})$ represents the weight of importance PDF $\pi(x_k|x_{0:k-1}^{(i)}, z_{1:k})$ after normalization of several sample particles, and $\delta(*)$ represents the Dirac function.

### B. THEORY DEDUCTION OF THE CSPF

The particle set $\{X_k^\bullet(i)\}_{i=1}^n = \{x_j^\circ(i) : j = k, \cdots, k+L; x_j'(i) : j = k+L+1, \cdots, k+L+l\}_{i=1}^n$ of the state combination trajectory from time $k$ to $k+L+l$ is selected. Among them, $x_j^\circ(i)$ follows *SIS* filtering, $x_j'(i)$ complies with the *GPF* prediction, and $L$ and $l$ are the filtering and prediction trajectory lengths, respectively. Because the real state of the actual system is unknown, the trajectory consistency of the spatial state is characterized by the observation likelihood function. The corresponding observation likelihood trajectory $\{Z_k^\bullet(i)\}_{i=1}^n = \{z_j^\circ(i) : j = k, \cdots, k+L; z_j'(i) : j = k+L+1, \cdots, k+L+l\}_{i=1}^n$ is solved using the observation equation

$$Z_k^\bullet(i) = h(X_k^\bullet(i), v_k) \tag{51}$$

While the observed likelihood trajectory of the real state is $\{Z_k\} = \{z_j : j = k, \cdots, k+L+l\}$. The cluster analysis method uses distance similarity [38] to measure the consistency of the state space trajectory. The distance similarity measure $D_k^\bullet$ of the observation likelihood trajectory between the real state and sampled particles is calculated as follows:

$$\begin{aligned} D_k^\bullet(i) &= dis(\{Z_k\}, \{Z_k^\bullet(i)\}_{i=1}^n) \\ &= \sqrt[\kappa]{\sum_{j=k}^{K+L} |y_j - y_j^\circ(i)|^\rho + \sum_{j=k+L+1}^{K+L+l} |y_j - y_j'(i)|^\kappa} \end{aligned} \tag{52}$$

where $dis(*)$ represents the distance similarity function, which satisfies $dis(*) \geq 0$, and $\kappa$ is the measurement type factor.

To enhance the algorithm output of reliability and robustness, the above formula is exponentially transformed to

$$D_k(i) = e^{\lambda \times D_k^\bullet(i)}, \quad i = 1, \cdots, n \tag{53}$$

where $\lambda$ is the reliable gradient factor. The first-order Markov process is updated and modified using the observation information similarity between the current *SIS* filter and the future multistage *GPF* prediction. The importance weights $W_k^\bullet(i)$ and $W_{k+L+l}^\bullet(i)$ corresponding to times $k$ and $k+L+l$ can be calculated as follows:

$$W_k^\bullet(i) = D_k^{-1}(i) \times p_v(Z_k - h(X_k^\bullet(i), v_k)), \ i = 1, \cdots, n \tag{54}$$

$$W_{k+L+l}^\bullet(i) = D_k^{-1}(i) \times p_v(Z_{k+L+l} - h(X_{k+L+l}^\bullet(i), v_k)), \quad i = 1, \cdots, n \tag{55}$$

where $p_v(*)$ is the PDF of the observation likelihood function.

### C. CONVERGENCE OF THE CSPF

Definition 3.2 Assuming that $\rho$ and $\Phi$ represent the probability measure and any bounded test function, respectively $\partial$ and $\Theta$ represent two types of independent variables of any function, and the kernel function $K$ satisfies the first-order Markov process, the following calculation method is defined:

$$(\rho, \Phi) \triangleq \int \Phi(x)\rho(\mathrm{d}x) \tag{56}$$

$$\rho K(\partial) \triangleq \int K(\partial|x)\rho(\mathrm{d}x) \tag{57}$$

$$K\Phi(x) \triangleq \int \Phi(\Theta)K(\mathrm{d}\Theta|x) \tag{58}$$

Then, the system state probability measure $\varpi_{j:k|m}(dx_{j:k})$ is defined as

$$\varpi_{j:k|m}(dx_{j:k}) \triangleq p(x_{k:l}|z_{1:m}) \tag{59}$$

Bayesian filtering formula (Prediction-Update) for any bounded test function $\Phi$, $\Re^{n_x}$ is the *Borelσ – algebra* set of system state $x$ on n-dimensional Euclidean space $n_x$. Through the above definition method and referring to formula (23), it can be revised as follows:

$$\begin{aligned} &(\varpi_{k|k-1}, \Phi) \\ &= \int_{\Re^{n_x}} p(x_k|z_{1:k-1})\Phi(x_k)\mathrm{d}x_k \\ &= \int_{\Re^{n_x}} \left[\int_{\Re^{n_x}} K(x_k|x_{k-1})p(x_{k-1}|z_{1:k-1})\mathrm{d}x_{k-1}\right]\Phi(x_k)\mathrm{d}x_k \\ &= \int_{\Re^{n_x}} p(x_{k-1}|z_{1:k-1})\left[\int_{\Re^{n_x}} K(x_k|x_{k-1})\Phi(x_k)\mathrm{d}x_k\right]\mathrm{d}x_{k-1} \\ &= (\varpi_{k-1|k-1}, K\Phi) \qquad \text{(Prediction)} \end{aligned} \tag{60}$$

Within the range of measure set $\Gamma(\Re^{n_x}) \to \Gamma(\Re^{n_x})$, the prediction mapping relationship $a_k(*)$ can also be used to represent the prediction process

$$\varpi_{k|k-1} = a_k(\varpi_{k-1|k-1}) \tag{61}$$

$$(a_k(\nu), \Phi) = \iint_{\Re^{n_x}} \nu K(dx_k|x_{k-1})\Phi(x_k)(dx_{k-1}) = (\nu, K\Phi) \tag{62}$$

where $\nu$ represents any form of probability measure, and $\nu \in \Gamma(\Re^{n_x})$.

Similarly, the reference update process formula (24) can be updated as follows:

$$\begin{aligned}(\varpi_{k|k}, \Phi) &= \int_{\Re^{n_x}} p(x_k|z_{1:k})\Phi(x_k)\mathrm{d}x_k \\ &= \frac{\int_{\Re^{n_x}} B(z_k|x_k)p(x_k|z_{1:k-1})\Phi(x_k)\mathrm{d}x_k}{\int_{\Re^{n_x}} B(z_k|x_k)p(x_k|z_{1:k-1})\mathrm{d}x_k} \\ &= \frac{(\varpi_{k|k-1}, B\Phi)}{(\varpi_{k|k-1}, B)} \quad \text{(Update)} \end{aligned} \tag{63}$$

Within the range of measure set $\Gamma(\Re^{n_x}) \rightarrow \Gamma(\Re^{n_x})$, the update mapping relationship $b_k(*)$ can also be used to represent the update process

$$\varpi_{k|k} = b_k(\varpi_{k|k-1}) \tag{64}$$

$$(b_k(\nu), \Phi) = (\nu, B\Phi)/(\nu, B) \tag{65}$$

It can be concluded that the whole Bayesian filtering process is expressed as

$$\varpi_{k|k} = b_k(\varpi_{k|k-1}) \triangleq b_k \odot a_k(\varpi_{k-1|k-1}) \tag{66}$$

where $\odot$ represents the composite mapping operator.

Through the above analysis, it can be concluded that the PF is based on Bayesian theory and a Monte Carlo random idea to generate a sampling disturbance function $c^n$. Then, the whole filtering process can be expressed as

$$\varpi^n_{k|k} = b_k \odot c^n \odot a_k(\varpi^n_{k-1|k-1}) \tag{67}$$

where $\varpi^n_{k|k}$ is the probability measure under random disturbance of Monte Carlo sampling, and $\varpi_{k|k}$ is the probability measure of the actual system state. When $n \rightarrow \infty$, the state estimation will converge to the actual system state [41], [42], i.e.,

$$\lim_{n\rightarrow\infty} c^n(a_k(\varpi^n_{k-1|k-1})) = c^n(a_k(\varpi_{k-1|k-1})) \tag{68}$$

In this case, the CSPF algorithm uses the cluster analysis method to measure the trajectory similarity of multistage observation information, which is adopted to compensate for the proposed distribution $\pi(x_k|x_{k-1}, z_k)$ in the *SIS* process.

$$\pi(x_k|x_{k-1}, z_k) = D_k(i)K(x_k|x_{k-1}) \tag{69}$$

Then, the sequential importance weight calculation is updated and corrected

$$W_k(i) \propto D_k^{-1}(i)B(z_k|x_k) = \hat{B}(z_k|x_k) \tag{70}$$

By substituting into formula (65), the update corrected process of the CSPF algorithm can be obtained

$$(\hat{b}_k(\nu_n), \Phi) = (\nu_n, \hat{B}\Phi)/(\nu_n, \hat{B}) \tag{71}$$

where $\hat{b}_k$ represents the update mapping relationship of the CSPF algorithm, the random measure $\nu_n$ of Monte Carlo sampling satisfies $\lim_{n\rightarrow\infty} \nu_n = \nu$, and $\nu \in \Gamma(\Re^{\nu})$. Referring to formulas (67) and (68), the state estimation measure $\hat{\varpi}^n_{k|k}$ of the CSPF algorithm can be expressed as

$$\hat{\varpi}^n_{k|k} = \hat{b}_k \odot c^n \odot a_k(\hat{\varpi}^n_{k-1|k-1}) = \hat{b}_k \odot c^n(a_k(\hat{\varpi}^n_{k-1|k-1})) \tag{72}$$

At time $k$, the probability measure of the Bayesian prediction stage is $a_k$, and the observed likelihood PDF $B(z_k|x_k)$ satisfies the premise of being continuous, bounded and strictly positive within the range $x_k \in \Re^{n_x}$ of state variables. Combined with the probability measures $\nu_j : \Omega \rightarrow \Re^{\nu}$ of i.i.d. random variables corresponding to the measure $\nu$ satisfy $\forall\Phi \in \Lambda$ and $\Lambda = \{\Phi_i\}_{i>0} \in \mathbb{C}_b(\Re^{n_x})$, the expected value of the difference between the measure of the Bayesian prediction stage and the real stage can be obtained

$$\begin{aligned} &E\left[((c^n(a_k), \Phi_i) - (a_k, \Phi_i))^4\right] \\ &= \frac{1}{n^4}E\left[\left(\sum_{j=1}^{n}(\Phi_i(\nu_j) - (a_k, \Phi_i))\right)^4\right] \\ &= \frac{1}{n^4}\sum_{j=1}^{n}E\left[(\Phi_i(\nu_j) - (a_k, \Phi_i))^4\right] \\ &= \frac{4}{n^4}\sum_{\substack{j_1,j_2=1 \\ j_1\neq j_2}}^{n}E\left[(\Phi_i(\nu_{j1}) - (a_k, \Phi_i))^2(\Phi_i(\nu_{j2}) - (a_k, \Phi_i))^2\right] \\ &\leq \frac{3n(n-1)\|2\Phi_i\|^4 + n\|2\Phi_i\|^4}{n^4} \leq \frac{48\|\Phi_i\|^4}{n^2} \end{aligned} \tag{73}$$

where $E[*]$ is the solution function of the set expectation, $\|*\|$ is equipped with the supremum norm in the domain $\mathbb{C}_b(\Re^{n_x})$, and $\|\Phi_i\| \triangleq \sup_{x\in\Re^{n_x}} |\Phi(\nu)|$. The summed expectation of the particle number of Monte Carlo sampling from 1 to $\infty$ is

$$E\left[\sum_{n=1}^{\infty}((c^n(a_k), \Phi_i) - (a_k, \Phi_i))^4\right] \leq 48\|\Phi_i\|^4\sum_{n=1}^{\infty}\frac{1}{n^2} < \infty \tag{74}$$

Hence,

$$\sum_{n=1}^{\infty}\left((c^n(a_k), \Phi_i) - (a_k, \Phi_i)\right)^4 < \infty \tag{75}$$

It is concluded that the measurement relationship of the prediction stage at time $k$ can be expressed as

$$\lim_{n\rightarrow\infty}((c^n(a_k), \Phi_i) - (a_k, \Phi_i)) = 0 \tag{76}$$

Combined with formulas (68) and (72), the prediction stage of the CSPF method under the random disturbance $c^n$ influence of Monte Carlo sampling can be expressed as

$$\lim_{n\rightarrow\infty} c^n\left(a_k(\hat{\varpi}^n_{k-1|k-1})\right) = a_k(\varpi_{k-1|k-1}) \tag{77}$$

For arbitrary measure $\nu_n \in \Gamma(\Re^{n_x})$ and function $\Phi$, referring to formula (71) and limit solution theory, the update correction process can be expressed as

$$\begin{aligned}\lim_{n\rightarrow\infty}(\hat{b}_k(\nu_n), \Phi) &= \frac{\lim_{n\rightarrow\infty}(\nu_n, \hat{B}\Phi)}{\lim_{n\rightarrow\infty}(\nu_n, \hat{B})} \\ &= \frac{\lim_{n\rightarrow\infty} D_k^{-1}(i)(\nu_n, B\Phi)}{\lim_{n\rightarrow\infty} D_k^{-1}(i)(\nu_n, B)} \\ &= \frac{(\nu_n, B\Phi)}{(\nu_n, B)} = (b_k(\nu), \Phi) \end{aligned} \tag{78}$$

Substituting the above results into formulas (63) and (64), it can be concluded that the CSPF algorithm has the same measure expression as Bayesian filtering in the update stage

$$\lim_{n\to\infty} \hat{b}_k(v_n) = b_k(v) \tag{79}$$

Combining formulas (66), (72), (77) and (79), we can obtain

$$\begin{aligned}\lim_{n\to\infty} \hat{\varpi}^n_{k|k} &= \lim_{n\to\infty} \hat{b}_k \odot c^n \odot a_k(\hat{\varpi}^n_{k-1|k-1}) \\ &= b_k \odot a_k(\varpi_{k-1|k-1}) = \varpi_{k|k}\end{aligned} \tag{80}$$

Through the above derivation, it can be concluded that under the random disturbance $c^n$ influence of Monte Carlo sampling, the improved particle filter algorithm based on cluster similarity to measure the consistency of the state trajectory can still converge to the actual system state [43]. Theorem 3.1 is proved.

## REFERENCES

[1] D. Lee, N. Ku, T.-W. Kim, J. Kim, K.-Y. Lee, and Y.-S. Son, "Development and application of an intelligent welding robot system for shipbuilding," *Robot. Comput.-Integr. Manuf.*, vol. 27, no. 2, pp. 377–388, Apr. 2011.
[2] O. Kermorgant, "A magnetic climbing robot to perform autonomous welding in the shipbuilding industry," *Robot. Comput.-Integr. Manuf.*, vol. 53, pp. 178–186, Oct. 2018.
[3] A. Zych, "Programming of welding robots in shipbuilding," *Proc. CIRP*, vol. 99, pp. 478–483, May 2021.
[4] S. Chen, T. Qiu, T. Lin, and Y. Wu, "On intelligentized technologies for modern welding manufacturing," *Chin. J. Mech. Eng.*, vol. 16, no. 4, pp. 367–370, Dec. 2003.
[5] K. Guan, Y. Sun, G. Yang, and X. Yang, "Knowledge acquisition and reasoning model for welding information integration based on CNN and knowledge graph," *Electronics*, vol. 12, no. 6, p. 1275, Mar. 2023.
[6] P. Yao, K. Zhou, H. Lin, Z. Xu, and S. Yue, "Exploration of weld bead forming rule during double-pulsed GMAW process based on grey relational analysis," *Materials*, vol. 12, no. 22, p. 3662, Nov. 2019.
[7] A. Ikram and H. Chung, "Numerical simulation of arc, metal transfer and its impingement on weld pool in variable polarity gas metal arc welding," *J. Manuf. Processes*, vol. 64, pp. 1529–1543, Apr. 2021.
[8] S. Kou and Y. Wang, "Weld pool convection and its effect," *Weld. J.*, vol. 65, no. 3, pp. 63–70, Mar. 1986.
[9] H.-Y. Du, Y.-H. Wei, W.-X. Wang, W.-M. Lin, and D. Fan, "Numerical simulation of temperature and fluid in GTAW-arc under changing process conditions," *J. Mater. Process. Technol.*, vol. 209, no. 8, pp. 3752–3765, Apr. 2009.
[10] H. J. Aval, A. Farzadi, S. Serajzadeh, and A. H. Kokabi, "Theoretical and experimental study of microstructures and weld pool geometry during GTAW of 304 stainless steel," *Int. J. Adv. Manuf. Technol.*, vol. 42, nos. 11–12, pp. 1043–1051, Jun. 2009.
[11] G. Xu, J. Hu, and H. L. Tsai, "Three-dimensional modeling of the plasma arc in arc welding," *J. Appl. Phys.*, vol. 104, no. 10, Nov. 2008, Art. no. 103301.
[12] D. J. Kotecki, D. L. Cheever, and D. G. Howden, "Mechanism of ripple formation during welding solidification," *Weld. J.*, vol. 51, no. 8, pp. 386–391, Aug. 1972.
[13] Q. Wang, J. Zhang, and C. Yang, "Detection of weld full penetration signals of a travelling arc in GTAW process," *Trans. China Weld. Inst.*, vol. 11, no. 3, pp. 175–180, Oct. 1990.
[14] R. P. Singh, S. Dubey, A. Singh, and S. Kumar, "A review paper on friction stir welding process," *Mater. Today*, vol. 38, pp. 6–11, Jun. 2021.
[15] D. Pathak, R. P. Singh, S. Gaur, and V. Balu, "To study the influence of process parameters on weld bead geometry in shielded metal arc welding," *Mater. Today*, vol. 44, pp. 39–44, Apr. 2021.
[16] R. Li, M. Dong, and H. Gao, "Prediction of bead geometry with changing welding speed using artificial neural network," *Materials*, vol. 14, no. 6, p. 1494, Mar. 2021.
[17] A. Gadagi and N. R. Mandal, "Heat source modeling for FCAW of fillet joints using artificial neural networks," *J. Ship Prod. Des.*, vol. 35, no. 1, pp. 80–87, Feb. 2019.
[18] X. Huang and S. Chen, "SVM-based fuzzy modeling for the arc welding process," *Mater. Sci. Eng., A*, vol. 427, nos. 1–2, pp. 181–187, Jul. 2006.
[19] Z. Feng and C. Liu, "An approach of ship welding production design based on rough set knowledge modeling," *Mar. Technol.*, vol. 43, no. 1, pp. 58–62, Feb. 2015.
[20] Z. Jiao, Z. Feng, S. Chen, H. Chen, and J. Yu, "An approximate inference scheme based on distance-induced relations: Weld forming prediction," *IEEE Access*, vol. 9, pp. 62820–62836, 2021.
[21] Z.-Q. Feng, Z.-Q. Jiao, S.-B. Chen, J.-F. Han, X.-X. Han, R.-D. Yang, and C.-G. Liu, "On rough set-based modeling and with application to process decision for forming plate by line heating," *J. Ship Prod. Des.*, vol. 35, no. 03, pp. 289–296, Aug. 2019.
[22] Z. Zhou, Y. Tan, and X. Liu, "State estimation of dynamic systems with sandwich structure and hysteresis," *Mech. Syst. Signal Process.*, vol. 126, pp. 82–97, Jul. 2019.
[23] Y. Huang, K. Wang, and X. Zhao, "Translation invariant wavelet denoising of $CO_2$ gas shielded arc welding electrical signal," *J. Mech. Eng.*, vol. 54, no. 8, pp. 95–100, Apr. 2018.
[24] V. Kumar, S. K. Albert, and N. Chandrasekhar, "Signal processing approach on weld data for evaluation of arc welding electrodes using probability density distributions," *Measurement*, vol. 133, pp. 23–32, Feb. 2019.
[25] Z. Jin, H. Li, G. Jia, and H. Gao, "Dynamic nonlinear modeling of 3D weld pool surface in GTAW," *Robot. Comput.-Integr. Manuf.*, vol. 39, pp. 1–8, Jun. 2016.
[26] Z. Zhou and X. Liu, "State and fault estimation of sandwich systems with hysteresis," *Int. J. Robust Nonlinear Control*, vol. 28, no. 13, pp. 3974–3986, Apr. 2018.
[27] N. Lin, R. Chi, and B. Huang, "Data-driven recursive least squares methods for non-affined nonlinear discrete-time systems," *Appl. Math. Model.*, vol. 81, pp. 787–798, May 2020.
[28] P. Zhang and A. M. Krieger, "Appropriate penalties in the final prediction error criterion: A decision theoretic approach," *Statist. Probab. Lett.*, vol. 18, no. 3, pp. 169–177, Oct. 1993.
[29] S. Chen, Y. Lou, L. Wu, and D. Zhao, "Intelligent methodology for sensing, modeling and control of pulsed GTAW: Part 1—Bead-on-plate welding," *Weld. J.*, vol. 79, no. 6, pp. 151–163, Jun. 2000.
[30] M. S. Arulampalam, S. Maskell, N. Gordon, and T. Clapp, "A tutorial on particle filters for online nonlinear/non-Gaussian Bayesian tracking," *IEEE Trans. Signal Process.*, vol. 50, no. 2, pp. 174–188, Feb. 2002.
[31] X. Fu and Y. Jia, "An improvement on resampling algorithm of particle filters," *IEEE Trans. Signal Process.*, vol. 58, no. 10, pp. 5414–5420, Oct. 2010.
[32] P. H. Peskun, "Optimum Monte–Carlo sampling using Markov chains," *Biometrika*, vol. 60, no. 3, pp. 607–612, Dec. 1973.
[33] L. Zhang, Y. Zhu, P. Shi, and Y. Zhao, "Resilient asynchronous $H_\infty$ filtering for Markov jump neural networks with unideal measurements and multiplicative noises," *IEEE Trans. Cybern.*, vol. 45, no. 12, pp. 2840–2852, Dec. 2015.
[34] N. J. Gordon, D. J. Salmond, and A. F. Smith, "Novel approach to nonlinear/non-Gaussian Bayesian state estimation," *IEE Proc. F, Radar Signal Process.*, vol. 140, no. 2, pp. 107–113, May 1993.
[35] M. Ahwiadi and W. Wang, "An adaptive particle filter technique for system state estimation and prognosis," *IEEE Trans. Instrum. Meas.*, vol. 69, no. 9, pp. 6756–6765, Sep. 2020.
[36] R. Havangi, "Robust evolutionary particle filter," *ISA Trans.*, vol. 57, pp. 179–188, Jul. 2015.
[37] A. Salarpour and H. Khotanlou, "Direction-based similarity measure to trajectory clustering," *IET Signal Process.*, vol. 13, no. 1, pp. 70–76, Feb. 2019.
[38] H. He and Y. Tan, "Unsupervised classification of multivariate time series using VPCA and fuzzy clustering with spatial weighted matrix distance," *IEEE Trans. Cybern.*, vol. 50, no. 3, pp. 1096–1105, Mar. 2020.
[39] Z. Zhou, Y. Tan, Y. Xie, and R. Dong, "State estimation of a compound non-smooth sandwich system with backlash and dead zone," *Mech. Syst. Signal Process.*, vol. 83, pp. 439–449, Jan. 2017.
[40] J. Candy, "Bootstrap particle filtering," *IEEE Signal Process. Mag.*, vol. 24, no. 4, pp. 73–85, Jul. 2007.

[41] Z. Jiao, Z. Feng, N. Lv, W. Liu, and H. Qin, "Improved particle filter using clustering similarity of the state trajectory with application to nonlinear estimation: Theory, modeling, and applications," *J. Sensors*, vol. 2021, May 2021, Art. no. 9916339.
[42] H. Zhou, Z. Deng, Y. Xia, and M. Fu, "A new sampling method in particle filter based on Pearson correlation coefficient," *Neurocomputing*, vol. 216, pp. 208–215, Dec. 2016.
[43] Z. Zhou, Y. Tan, and P. Shi, "Fault detection of a sandwich system with dead-zone based on robust observer," *Syst. Control Lett.*, vol. 96, pp. 132–140, Oct. 2016.

**ZIQUAN JIAO** received the M.S. degree in design and manufacture of ships and marine structures from the Dalian University of Technology (DUT), Dalian, China, in 2013. He is currently pursuing the Ph.D. degree in mechanical engineering with the Guilin University of Electronic Technology (GUET), Guilin, China. Since December 2017, he has been an Assistant Researcher with the Guangxi Ship Digital Design and Advanced Manufacturing Research Center of Engineering Technology, Beibu Gulf University. His current research interests include intelligent manufacturing technology and artificial intelligence.

**XINGYU GAO** received the Ph.D. degree in measure technology and instrument from Tianjin University, China, in 2010. From 2008 to 2009, he was a Joint Ph.D. Student with Swinburne University, Australia. He is currently a Professor and a Ph.D. Supervisor with the School of Mechanical and Electrical Engineering, Guilin University of Electronic Technology. He is also the Chair of the School of Mechanical and Electrical Engineering, Guilin University of Electronic Technology, and the Associate Chair of the Shenzhen Institute on Electronic Information and Advanced Manufacture Technology, Guilin University of Electronic Technology. He has directed over ten projects. He has published over 30 papers in some international journals and conferences. His current research interests include industrial detection by computer vision, robot technology, and intelligent manufacturing. As for the part-time academic, he is an Associate Chair of the Guangxi Mechanical Engineering Society.

**ZHIQIANG FENG** received the Ph.D. degree in ship design and manufacturing from Shanghai Jiao Tong University, Shanghai, China, in 2012. He is currently a Professor with the School of Electronics and Information Engineering, Beibu Gulf University. His research interests include digital shipbuilding and advanced manufacturing technology.

**TONGSHUAI YANG** received the bachelor's degree from Heze University, Heze, China, in 2021. He is currently pursuing the master's degree with the School of Mechanical and Marine Engineering, Beibu Gulf University. His research interests include signal processing, advanced manufacturing technology, and welding process modeling.

**SHANBEN CHEN** (Senior Member, IEEE) received the Ph.D. degree in control theory and application from the Harbin University of Science and Technology, Harbin, China, in 1991. He is currently a Professor with the School of Materials Science and Engineering, Shanghai Jiao Tong University, and the Director of the Robot Welding Intelligent Technology Laboratory. His research interests include soft computing, welding process intelligent control, and uncertain system robust control theory.

**WENJING LIU** received the M.S. degree from Guangxi University, Nanning, China, in 2014. She is currently pursuing the Ph.D. degree with Saitama University, Saitama, Japan. She is the author of more than three articles. Her research interests include mathematical statistics, clustering analysis, and data driven.